4. THE TROPICS—H. J. Diamond, Ed.

a. *Overview*—H. J. Diamond

This tropics section consists of five topics: 1) ENSO and the tropical Pacific; 2) the MJO; 3) TC activity for the 2008 season in seven basins: the North Atlantic, eastern North Pacific, northwest Pacific, north Indian and south Indian, South Pacific, and Australia; 4) ITCZ behavior in the Pacific and Atlantic basins; and 5) the IOD.

The year was characterized by fluctuating conditions throughout the tropical Pacific that began with a strong La Niña episode that ended in June. This was followed by ENSO-neutral conditions during the middle and latter half of the year, and a return to La Niña conditions late in December. The predominant La Niña conditions had significant impacts on the activity of the Atlantic and northeast Pacific TC seasons.

The 2008 Atlantic hurricane season was the 14th busiest on record and significantly more active than the 2006 and 2007 seasons. Conversely, activity in the northwest Pacific was considerably below normal during 2008. While activity in the north Indian Ocean was only slightly above average, the season was punctuated by Cyclone Nargis, which was the seventh-strongest cyclone ever in the basin.

Since the weak negative IOD in 2005, there have been three consecutive seasons from 2006–08 with a positive IOD.

b. *ENSO and the tropical Pacific*—M. L'Heureux, G. Bell, and M. Halpert

1) Oceanic conditions

ENSO is a coupled ocean–atmosphere phenomenon centered in the equatorial Pacific Ocean. ENSO features two opposing phases, El Niño and La Niña, which are responsible for considerable interannual climate variability in the global tropics and mid-to-high latitudes. NOAA defines these ENSO phases using the Niño-3.4 index, which reflects area-averaged SST anomalies between 5°N–5°S and 170°–120°W.

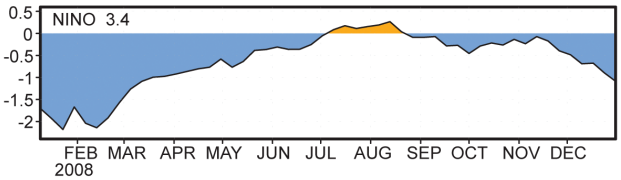

Fig. 4.1. Time series of SST anomalies (°C) in the Niño-3.4 region (5°N–5°S, 170°–120°W). Anomalies are departures from the 1971–2000 base period weekly means and are obtained from the adjusted OI dataset (Smith and Reynolds 1998).

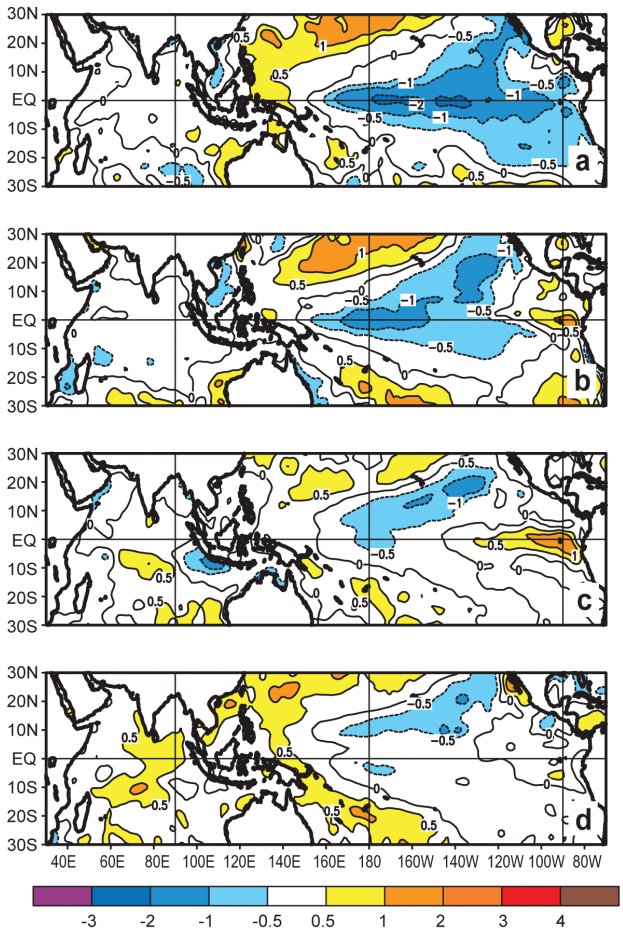

Fig. 4.2. SST anomalies (°C) during (a) Dec–Feb 2007–08, (b) Mar–May 2008, (c) Jun–Aug 2008, and (d) Sep–Nov 2008. Anomalies are departures from the 1971–2000 adjusted OI climatology (Smith and Reynolds 1998).

El Niño occurs when the 3-month running mean value of the Niño-3.4 index (ONI) is greater than or equal to +0.5°C, while La Niña occurs when the ONI is less than or equal to −0.5°C.

During 2008, conditions throughout the tropical Pacific reflected a strong La Niña episode that ended in June. This was followed by ENSO-neutral conditions during the middle and latter half of the year, and a return to La Niña conditions late in December (Fig. 4.1). During the peak of the event, the DJF 2007–08 ONI value was −1.4°C, with weekly values of the Niño-3.4 index dropping below −2°C. These measures indicated the strongest La Niña episode since 1999–2000.

The seasonal surface and subsurface temperature anomalies associated with the 2007–08 La Niña episode are summarized in Figs. 4.2, 4.3. SSTs during the peak of the event were at least 1°C below average

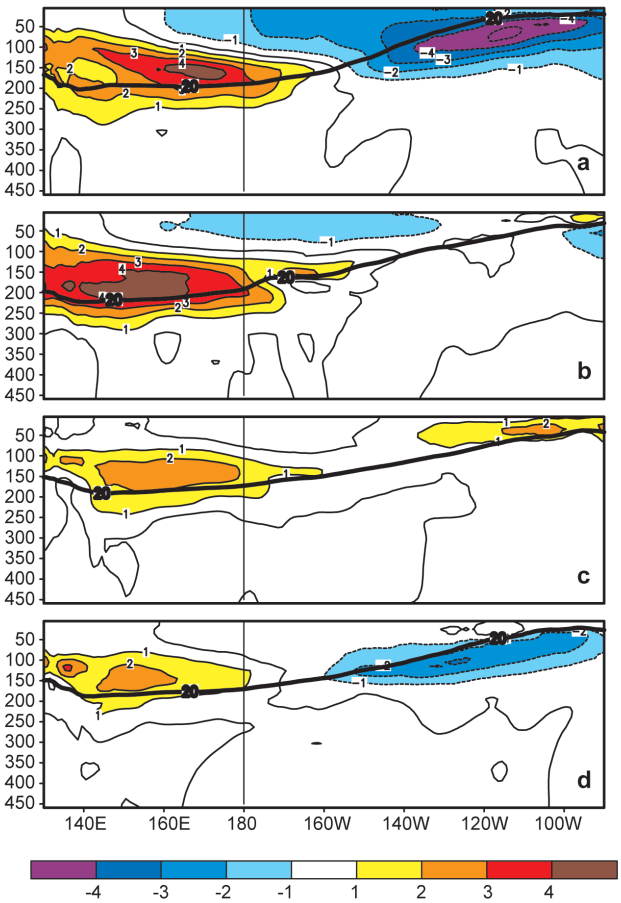

Fig. 4.3. Equatorial depth-longitude section of ocean temperature anomalies (°C) averaged between 5°N and 5°S during (a) Dec–Feb 2007–08, (b) Mar–May 2008, (c) Jun–Aug 2008, and (d) Sep–Nov 2008. The 20°C isotherm (thick solid line) approximates the center of the oceanic thermocline. The data are derived from an analysis system that assimilates oceanic observations into an oceanic GCM (Behringer et al. 1998). Anomalies are departures from the 1971–2000 period monthly means.

across the eastern half of the equatorial Pacific, with the largest departures (below –2°C) centered just east of the international date line and in the east-central Pacific (Fig. 4.2a).

The pattern of subsurface temperature anomalies illustrates the large vertical extent of the oceanic cooling during this period (Fig. 4.3a), with departures in some areas of the eastern Pacific at least 5°C below average. In the east-central and eastern Pacific, this cooling reflected an exceptionally shallow thermocline. In contrast, in the western half of the basin temperatures were significantly above average at thermocline depth (100–250 m), although negative anomalies resided close to the ocean surface (0–100 m). These subsurface temperature anomalies and the associated increased slope of the oceanic thermocline are typical of a mature La Niña.

During March–May 2008, a wide swath of below-average but somewhat weaker SST anomalies remained across the equatorial Pacific, except for the far eastern portion of the basin (Fig. 4.2b). The most significant evolution during this period occurred below the ocean surface, where the negative temperature anomalies in the east-central and eastern equatorial Pacific dissipated in response to a deepening of the oceanic thermocline (Fig. 4.3b). Subsequent additional warming and a westward expansion of positive SST anomalies in the eastern Pacific contributed to a rapid weakening of La Niña during May and June, and to the appearance of positive anomalies in the Niño-3.4 region by early July.

The dissipation of the anomalous subsurface temperature structure occurred in conjunction with oceanic Kelvin waves initiated during January and May (Fig. 4.7). These waves were triggered by low-level westerly wind events associated with MJO activity (section 4c). Major impacts of the final Kelvin wave in May included a weakening of the record-high (dating back to the start of the historical record in 1980) oceanic heat content anomalies in the western Pacific, and the development of positive surface (Fig. 4.2c) and subsurface (Fig. 4.3c) temperature anomalies in the eastern Pacific.

During SON 2008, near-average SSTs were evident throughout the equatorial Pacific Ocean (Fig. 4.2d). However, a more La Niña–like subsurface temperature pattern and thermocline structure became reestablished (Fig. 4.3d), which when combined with subsequent cooling of the SSTs, led to the reemergence of La Niña in December.

2) Atmospheric circulation

During DJF 2007–08 and MAM 2008 the below-average SSTs were strongly coupled to the atmosphere (Figs. 4.4a,b). For example, convection was suppressed over the central and east-central equatorial Pacific (brown shading), and enhanced over Indonesia and the far western Pacific (green shading). This pattern reflects a westward contraction of the equatorial convection toward the western Pacific and a complete disappearance of convection from the central Pacific.

These conditions were associated with enhanced easterly trade winds at 850 hPa (vectors, Figs. 4.4a,b) and anomalous upper-level westerly winds at 200 hPa (not shown) across the central and western equatorial Pacific Ocean, along with anomalous low-level westerly winds over the IO. This combination reflects

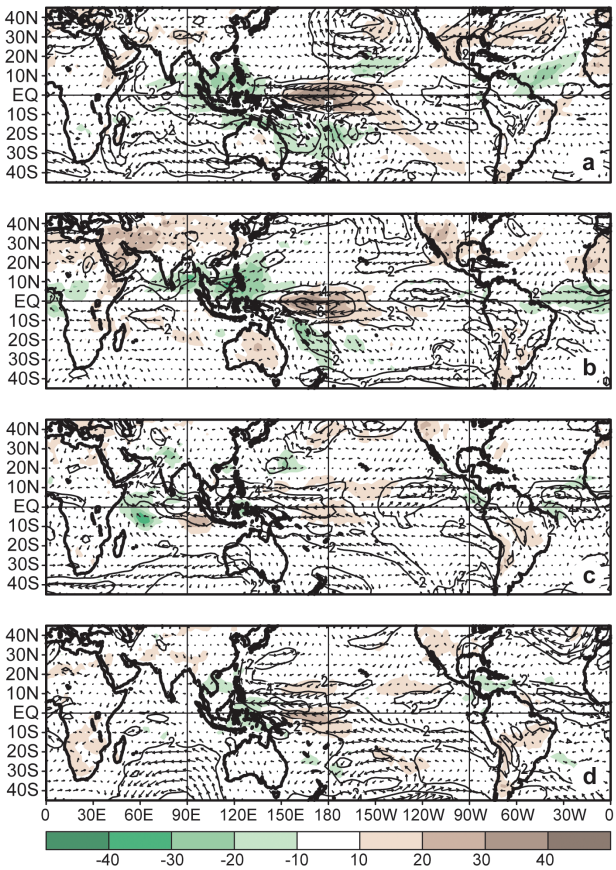

Fig. 4.4. Anomalous 850-hPa wind vector and speed (m s^{-1}) and anomalous OLR (shaded, W m^{-2}) during (a) Dec–Feb 2007–08, (b) Mar–May 2008, (c) Jun–Aug 2008, and (d) Sep–Nov 2008. Anomalies are departures from the 1979–95 period monthly means.

an enhanced equatorial Walker circulation that was confined to the western half of the Pacific Ocean, which is typical of La Niña.

In both hemispheres the subtropical circulation during DJF and MAM 2008 was also typical of La Niña, with cyclonic anomalies over the central and east-central Pacific and anticyclonic anomalies over Australasia (shading, Fig. 4.5a). This pattern reflected enhanced mid-Pacific troughs and a westward retraction of the subtropical ridges toward the western Pacific (contours, Fig. 4.5b). In the Northern Hemisphere, these conditions were associated with a westward retraction of the East Asian jet core, and a westward shift of the mean North American ridge to the eastern North Pacific and the mean Hudson Bay trough to western North America.

During JJA and SON the anomalous convection over the tropical Pacific weakened as La Niña dissipated (Figs. 4.4c,d). However, the low-level easterlies remained enhanced in the western and central Pacific Ocean, and convection remained suppressed near the date line.

3) La Niña impacts

Regional La Niña impacts during DJF 2007–08 and MAM 2008 included above-average rainfall across much of the Maritime Continent (e.g., Indonesia, Philippines, Malaysia, and Borneo) extending to northernmost portions of Australia. An enhanced and extreme southwestward displacement of the SPCZ in April 2008 contributed to increased rainfall over the southwestern Pacific Ocean, including significant flooding in Vanuatu (Island Climate Update 2008a).

Also consistent with La Niña, rainfall was enhanced in northeastern Brazil and in the South African monsoon region. Over the United States, La Niña led to drier-than-average conditions across much of the South and to increased precipitation in the Pacific Northwest and in the Ohio and Tennessee valleys. A persistent La Niña–like circulation contributed to an above-normal Atlantic hurricane season (section 4d2) and to below-average hurricane activity in the northeast Pacific (section 4d3).

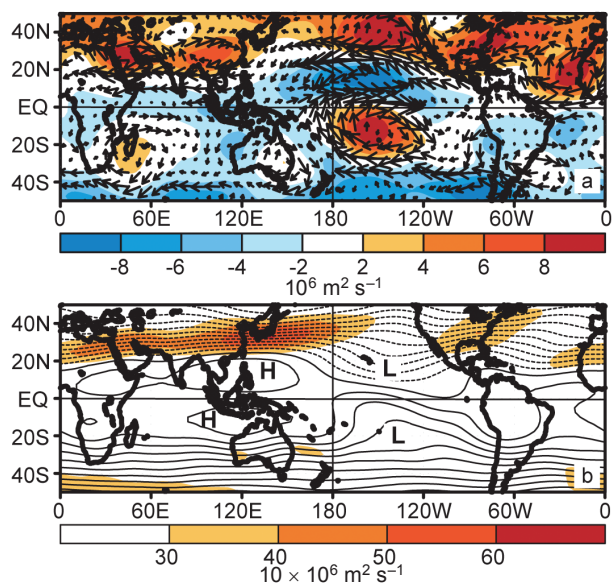

Fig. 4.5. 200-hPa circulation during Dec 2007–May 2008: (a) anomalous streamfunction (shading) and vector winds (m s^{-1}) and (b) total streamfunction (contours) and wind speed (shading). In (a), anomalous ridges are indicated by positive values (red) in the NH and negative values (blue) in the SH. Anomalous troughs are indicated by negative values in the NH and positive values in the SH. In (b), "L" indicates mid-Pacific trough and "H" indicates western Pacific subtropical ridge. Anomalies are departures from the 1971–2000 period monthly means.

c. *The Madden–Julian Oscillation*—J. Gottschalck and G. Bell

The MJO (Madden and Julian 1971, 1972, 1994) is a leading climate mode of tropical convective variability that occurs on intraseasonal time scales. The convective anomalies associated with the MJO often have the same spatial scale as ENSO, but differ in that they exhibit a distinct eastward propagation and generally traverse the globe in 30–60 days. The MJO can strongly affect the tropical and extratropical atmospheric circulation patterns, and sometimes produces ENSO-like anomalies (Mo and Kousky 1993; Kousky and Kayano 1994; Kayano and Kousky 1999). The MJO is often quite variable in a given year, with periods of moderate-to-strong activity sometimes followed by little or no activity. Overall, the MJO tends to be most active during neutral and weak ENSO periods and is often absent during strong El Niño events (Hendon et al. 1999; Zhang and Gottschalck 2002; Zhang 2005).

The MJO is seen by continuous propagation of 200-hPa velocity potential anomalies around the globe. A time–longitude section of this parameter shows three distinct periods during 2008 with at least moderate MJO activity (Fig. 4.6). These include 1) a continuation during January to early March of strong activity that began in late 2007, 2) moderate-to-strong activity from May through July, and 3) moderate-to-strong activity during September and October.

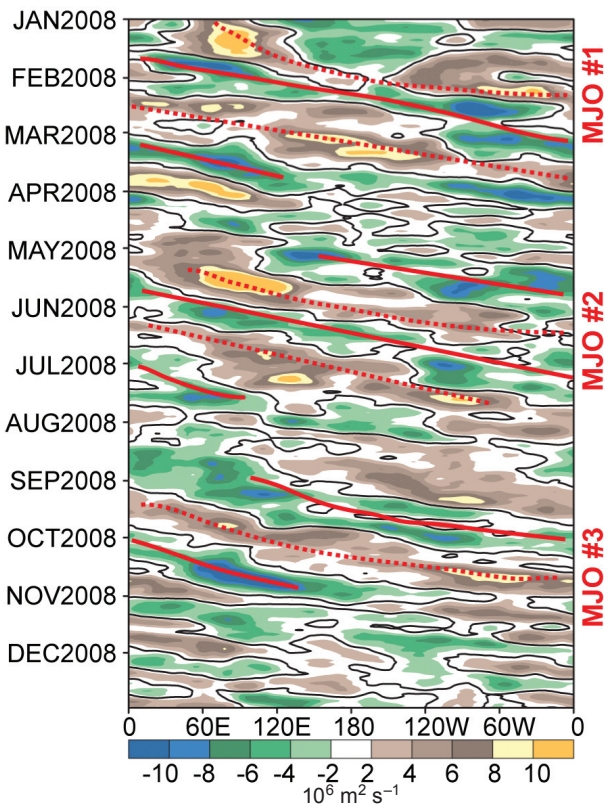

Fig. 4.6. Time–longitude section of filtered 200-hPa velocity potential anomaly (5°N–5°S) for 2008. Green (brown) shading represents anomalous divergence (convergence). Red lines highlight the MJO signal. The three MJO episodes are marked. Anomalies are departures from the 1971–2000 base period daily means.

The early and midyear activity was particularly interesting due to its interplay with La Niña. For example, during late December 2007, February–March and early May, the MJO and La Niña–related convective anomalies were in-phase, making it appear that La Niña and its associated downstream circulation anomalies were particularly strong. Conversely, during January, late May, and late June, the MJO and La Niña–related convective anomalies were out-of-phase, resulting in a masking of the underlying La Niña signals.

These varying climate conditions had several impacts in the Pacific/North American sector. During late December 2007, enhanced convection across Indonesia (in response to both the MJO and La Niña) resulted in a strong upper-level ridge over the high latitudes of the central North Pacific and an amplified trough over the eastern North Pacific. This circulation led to heavy precipitation across sections of central and Southern California in early January 2008, regions that normally receive little or no wintertime precipitation during La Niña.

Other periods when La Niña and the MJO were in-phase resulted in recurring jet stream patterns that favored exceptionally heavy precipitation events and eventual June flooding in the U.S. Midwest (see section 7b2). Also, consistent with the results of Mo (2000) and Maloney and Hartmann (2000), periods during 2008 with suppressed MJO-related convection near the date line were more La Niña–like and were associated with lower northeast Pacific and greater Atlantic hurricane activity.

Other interactions between the MJO and La Niña were related to two equatorial oceanic Kelvin waves that were triggered by the MJO during January and May 2008. In both events, the MJO completely masked La Niña's convective signal by producing suppressed convection over the Indian Ocean and Indonesia, and enhanced convection across the western Pacific and within the SPCZ. In each case, Kelvin waves were initiated by a dramatic weakening of the low-level easterly winds as the area of suppressed convection propagated into the western Pacific Ocean (dotted lines, Fig. 4.7).

The Kelvin wave triggered in January acted to lower the oceanic thermocline across the central and east-central equatorial Pacific, thereby substantially weakening the negative heat content anomalies as-

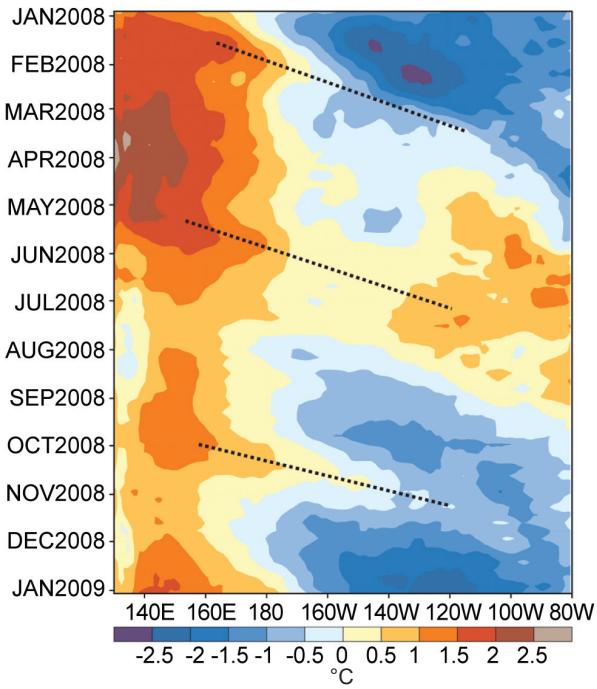

Fig. 4.7. Time–longitude section of the upper ocean (0–300 m) heat content anomaly (5°N–5°S) for 2008. Blue (yellow/red) shading indicates below- (above) average heat content. The downwelling phases (solid lines) of oceanic Kelvin waves are indicated. Anomalies are departures from the 1982–2004 base period pentad means.

sociated with La Niña. A similar warming due to the Kelvin wave triggered in May led to positive heat content anomalies across much of the Pacific basin during June and July, and to the end of La Niña (Fig. 4.3c).

A third equatorial Kelvin wave was triggered by the MJO in late September, again in response to the propagation of suppressed convection from the Indian Ocean to the western Pacific. This wave counteracted the anomalous cooling that was becoming reestablished across the central and east-central equatorial Pacific, and likely delayed the reemergence of La Niña until later in the year. The timing of La Niña's reemergence was also likely related to the opposite phase of the MJO in November, which featured significantly enhanced convection and stronger low-level easterlies over the western Pacific Ocean.

d. *Tropical cyclones*

1) Overview—H. J. Diamond

The global tallying of total storm numbers is always challenging and involves more than simply adding up basin totals, as there are a number of storms that cross basin boundaries. Averaged across all basins, the 2008 TC season (2007–08 in the Southern Hemisphere) saw a near-normal (1981–2000 base) number of tropical or NSs (≥ 34 kt) and a below-average number of HTCs (≥ 64 kt) and major HTCs (≥ 96 kt) than average. Globally, 96 NSs developed during 2008 (1 below average), and 46 became HTCs (9 below average). Of these, 20 (compared with 26 in 2006 and 18 in 2007) attained major/intense status (global average is 25.4).

The 2008 season was significantly above average in two basins (North Atlantic and south Indian); near to slightly above average in the NIO, and near to below average in the remaining basins (eastern North Pacific, northwest Pacific, southwest Pacific, and Australian region). The North Atlantic season was also active in terms of landfalling storms. The island of Hispaniola was affected by several storms (two direct hits); Cuba experienced two landfalls by major hurricanes; the continental United States experienced a total of six landfalling storms (including three hurricanes); and one hurricane made a very rare landfall in Nova Scotia, Canada. The NIO season was punctuated by a severe Category-5 storm (Cyclone Nargis), which was responsible for over 145,000 deaths and $10 billion (USD) in damages in Myanmar; Nargis is also ranked as the seventh-strongest storm ever in that basin. TC activity in the western North Pacific basin was also shifted farther westward and northward than normal and was unusually tranquil (see sidebar "Unusually Quiet West Pacific Typhoon Season Ends with a Dolphin Kick").

2) Atlantic basin—G. D. Bell, E. Blake, S. B. Goldenberg, T. Kimberlain, C. W. Landsea, R. Pasch, and J. Schemm

(i) Seasonal activity

The 2008 Atlantic hurricane season produced 16 NSs, of which 8 became Hs and 5 became MHs (J. Beven and D. Brown 2009, unpublished manuscipt). The 1950–2000 averages are 11 NSs, 6 Hs, and 2 MHs. For 2008 the ACE (Bell et al. 2000) was 167% of the median (Fig. 4.8).This value is the 14th most active since 1950 and is well into the above-normal range (see www.cpc.noaa.gov/products/outlooks/background_information.shtml), consistent with the ongoing active Atlantic hurricane era that began in 1995 (Goldenberg et al. 2001). It is the only season on record in which an MH existed in every month from July through November.

Consistent with other active seasons, 11 NSs formed in the MDR (Goldenberg and Shapiro 1996) during 2008 (green box, Fig. 4.9a). These systems accounted for seven Hs, all five MHs, and 88% of the ACE value. The season was also active in terms of landfalling NSs. The nations in and surrounding

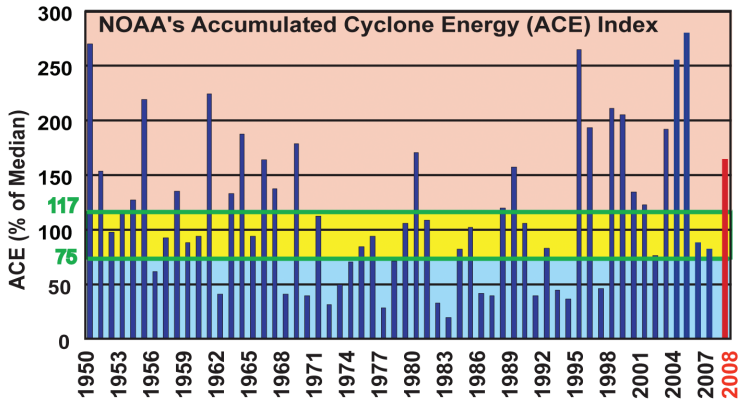

Fig. 4.8. ACE values expressed as percent of the 1950–2000 median value (87.5 × 10^4 kt^2). ACE is a wind energy index that measures the combined strength and duration of the NSs. ACE is calculated by summing the squares of the 6-hourly maximum sustained surface wind speed in knots (Vmax2) for all periods while the storm has at least TS strength. Pink, yellow, and blue shades correspond to NOAA's classifications for above-, near-, and below-normal seasons, respectively.

the Caribbean Sea were severely impacted by four TSs and four Hs. Cuba experienced three hurricane landfalls (including two MHs, Gustav and Ike), while Hispaniola was affected by several NSs including direct strikes by TS Fay and H Hanna. The continental United States was struck by three TSs and three Hs, with all but one TS making landfall along the Gulf Coast. Elsewhere, H Kyle made landfall in Nova Scotia, Canada.

(ii) SSTs

For the ASO climatological peak months of the season, SSTs were generally 0.5°–1.0°C above average in the MDR (Fig. 4.9a). The area-averaged SST anomaly in the MDR was 0.60°C, the fifth warmest since 1950 (Fig. 4.9b).

This warmth partly reflects the warm phase of the AMO (Enfield and Mestas-Nuñez 1999), which accompanied the 1995 transition to the active Atlantic phase of the tropical multidecadal signal (Goldenberg et al. 2001; Bell and Chelliah 2006). It also reflects reduced mixing and reduced evaporation from the ocean surface in response to weaker northeasterly trade winds (anomalous southwesterly flow) across the southern half of the MDR (Fig. 4.10a).

(iii) Atmospheric circulation

An interrelated set of atmospheric anomalies typical of recent active hurricane seasons (Landsea et al. 1998; Bell et al. 1999, 2000, 2004, 2006; Goldenberg et al. 2001; Bell and Chelliah 2006; Kossin and Vimont 2007) set the stage for the active 2008 hurricane season. These conditions are also known to greatly increase the probability of hurricane landfalls, as was seen in 2008.

During ASO 2008, weaker trade winds and high values of CAPE covered the southern half of the MDR (Fig. 4.10a), and sea level pressure was below average across the MDR (blue shading, Fig. 4.10b). These conditions were associated with a more northward position of the Atlantic ITCZ (section 4e2) and with an enhanced West African monsoon system.

The low-level westerly anomalies extended past 700 hPa, the approximate level of the African Easterly Jet, and were associated with a 5° northward shift of the AEJ core (black arrow) compared to climatology. As a result, the bulk of the African easterly wave energy (Reed et al. 1977) was often centered within the MDR. The AEJ also featured increased cyclonic shear along its equatorward flank, which dynamically favors stronger easterly waves and provides an inherent cyclonic rotation to their embedded convective cells.

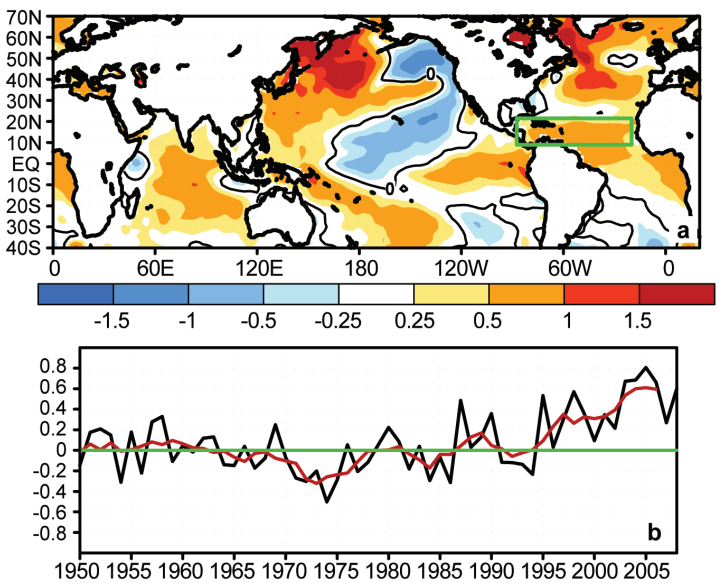

Fig. 4.9 (a) SST anomalies (°C) during Aug–Oct 2008. (b) Consecutive Aug–Oct area-averaged SST anomalies in the MDR. Red line shows the corresponding 5-yr running mean. Green box in (a) denotes the MDR. Anomalies are departures from the 1971–2000 monthly means.

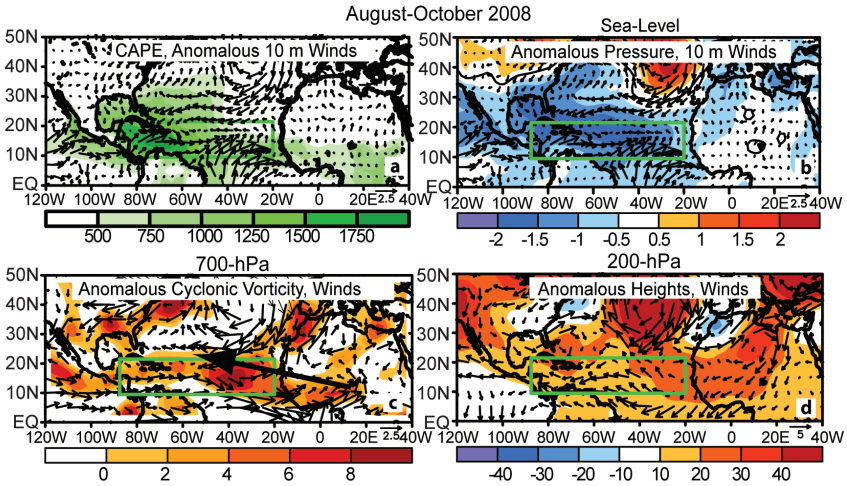

Fig. 4.10. Aug–Oct 2008: (a) total CAPE (J kg^{-1}) and anomalous vector winds (m s^{-1}) at 10 m; (b) anomalous sea level pressure (shading, hPa) and vector winds at 10 m; (c) 700-hPa anomalous cyclonic relative vorticity (shading) and vector winds, with thick arrow indicating the observed AEJ core; (d) 200-hPa anomalous heights and vector winds. Green boxes denote the MDR. Anomalies are departures from the 1971–2000 monthly means.

At 200 hPa, the wind and height anomalies reflected an enhanced upper-level ridge and a stronger, more westward extension of the tropical easterly jet (Fig. 4.10d). The result was weak (less than 8 m s^{-1}) vertical wind shear between 200 and 850 hPa across much of the MDR (shading, Fig. 4.11a), with the most anomalously weak shear spanning the central tropical Atlantic Ocean and Caribbean Sea (Fig. 4.11b).

This combination of conditions meant that many TSs developed from amplifying African easterly waves in an environment of below-average pressure and increased cyclonic shear. Those waves were also embedded within an extended region of weak vertical wind shear, which enabled further intensification as they moved westward over progressively warmer SSTs.

Two prominent climate phenomena can account for the interrelated set of anomalies associated with the 2008 Atlantic hurricane season. These are the ongoing active Atlantic phase of the tropical multidecadal signal and lingering La Niña signals.

(iv) Conditions associated with the ongoing active Atlantic hurricane era

2008 marks the 10th above-normal Atlantic hurricane season since the current high-activity era began in 1995. During 1995–2008 only the strong El Niño year of 1997 had below-normal activity. The increased activity since 1995 contrasts with the preceding low-activity era 1971–94, when half of the seasons were below normal and only three were above normal.

The transition to the current active era was associated with a phase change in the tropical multidecadal signal, which reflects the leading modes of tropical convective rainfall variability occurring on multidecadal time scales (Bell and Chelliah 2006; Bell et al. 2007). This signal highlights the convectively driven nature of the atmospheric anomalies across the central and eastern MDR, and links them to an east–west oscillation in anomalous convection between western Africa (Landsea and Gray 1992; Goldenberg and Shapiro 1996) and the Amazon basin. As seen in 2008, the combination of an enhanced West African monsoon and suppressed convection in the Amazon basin (Fig. 4.12a) is consistent with the ongoing high-activity era (Fig. 4.12b), as is the anomalous low-level inflow into the West African monsoon region

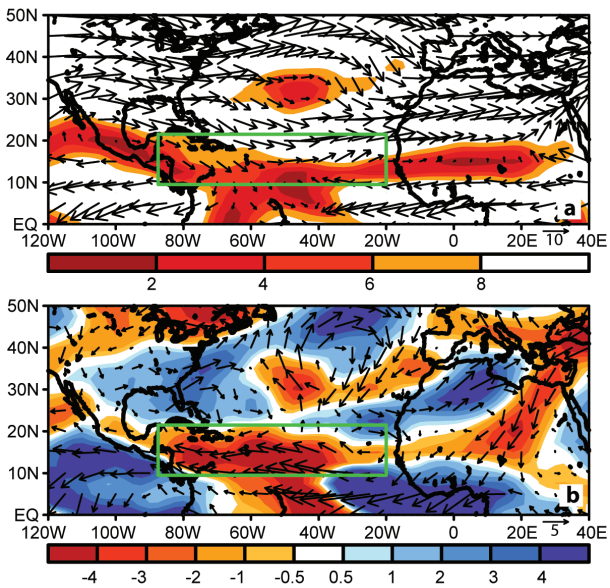

Fig. 4.11. Aug–Oct 2008: 200–850-hPa vertical wind shear magnitude (m s^{-1}) and vectors (a) total and (b) anomalies. In (a), shading indicates values below 8 m s^{-1}. In (b), red (blue) shading indicates below- (above) average magnitude of the vertical shear. Green boxes denote the MDR. Anomalies are departures from the 1971–2000 monthly means.

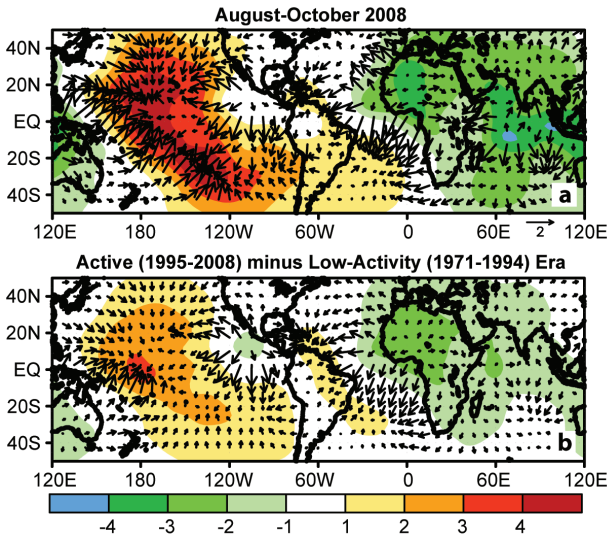

Fig. 4.12. 200-hPa velocity potential (shading) and divergent wind vectors (m s^{-1}): (a) Aug–Oct 2008 anomalies and (b) high-activity (1995–2008) period means minus low-activity (1971–94) period means. Anomalies are departures from the 1971–2000 monthly means.

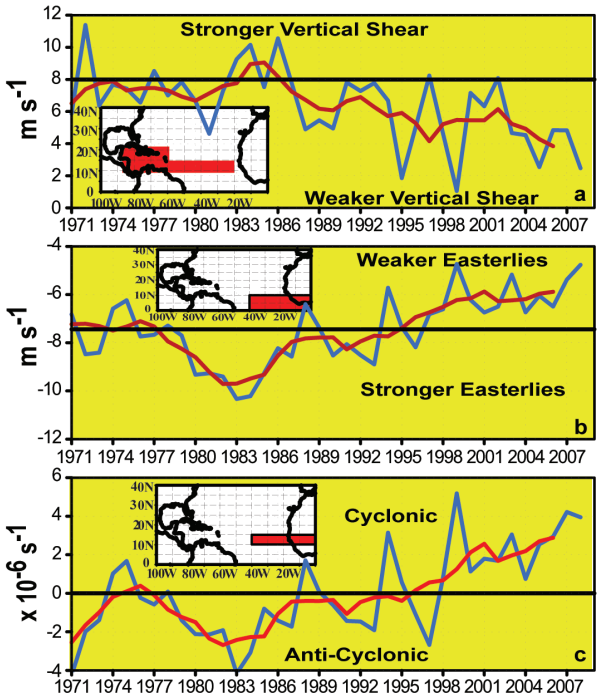

Fig. 4.13. Time series showing consecutive Aug–Oct values of area-averaged (a) 200–850-hPa vertical shear of the zonal wind (m s^{-1}), (b) 700-hPa zonal wind (m s^{-1}), and (c) 700-Pa relative vorticity (× 10^{-6} s^{-1}). Blue curves show unsmoothed values, and red curves show a 5-pt running mean of the time series. Averaging regions are shown in the insets.

(Fig. 4.11a) and enhanced upper-level outflow from that region (Figs. 4.10d, 4.12a).

Consistent with these conditions are dramatic differences in the vertical wind shear (Fig. 4.13a), 700-hPa zonal winds (Fig. 4.13b), and 700-hPa relative vorticity (Fig. 4.13c), within the MDR between the high-activity and low-activity era.

An enhanced West African monsoon system has major impacts on the 200-hPa Northern Hemispheric circulation, as seen in 2008 by the pronounced interhemispheric symmetry of streamfunction anomalies across the eastern subtropical Atlantic Ocean and Africa (Fig. 4.14a). This pattern reflects enhanced upper-level ridges in the subtropics of both hemispheres and a stronger tropical easterly jet, both of which have prevailed throughout this high-activity era (Fig. 4.14b) (Bell and Chelliah 2006).

(v) La Niña

La Niña acts to reduce the vertical wind shear in the western MDR, thus favoring increased Atlantic hurricane activity (Gray 1984). During 2008, SSTs in the Niño-3.4 region returned to normal in June (Fig. 4.1). However, tropical convection remained suppressed near the date line throughout ASO (e.g., Fig. 4.4c), which favored cyclonic anomalies at 200 hPa over the western subtropical Pacific and anticyclonic anomalies over the eastern subtropical Pacific and Caribbean Sea (Fig. 4.14a). The associated anomalous easterly winds extended from the eastern Pacific to the tropical Atlantic, and contributed to reduced vertical wind shear in the western MDR. Historically, the presence of these conditions during a high-activity era greatly increases the probability of an above-normal Atlantic hurricane season.

During 2008, the window of opportunity for TC formation widened, as the above circulation anomalies (Figs. 4.12–4.14) were present before the peak of the season. For example, a large area of anomalous upper-level divergence and enhanced convection (indicated by the core of negative velocity potential anomalies; Fig. 4.15a) was already present during April–June over the eastern tropical Atlantic Ocean and West Africa (Fig. 4.15a). Impacts from this anomalous convection can be seen in the pattern of 200-hPa streamfunction anomalies (Fig. 4.15b), which shows amplified ridges in the subtropics of both hemispheres flanking the region of enhanced convection. As shown by Bell et al. (2009), the associated upper-level easterly anomalies and reduced vertical wind shear contributed to the development of two TCs (including long-lived MH Bertha) within the MDR during July, a month when conditions are normally unfavorable for low-latitude TC formation (DeMaria et al. 2001).

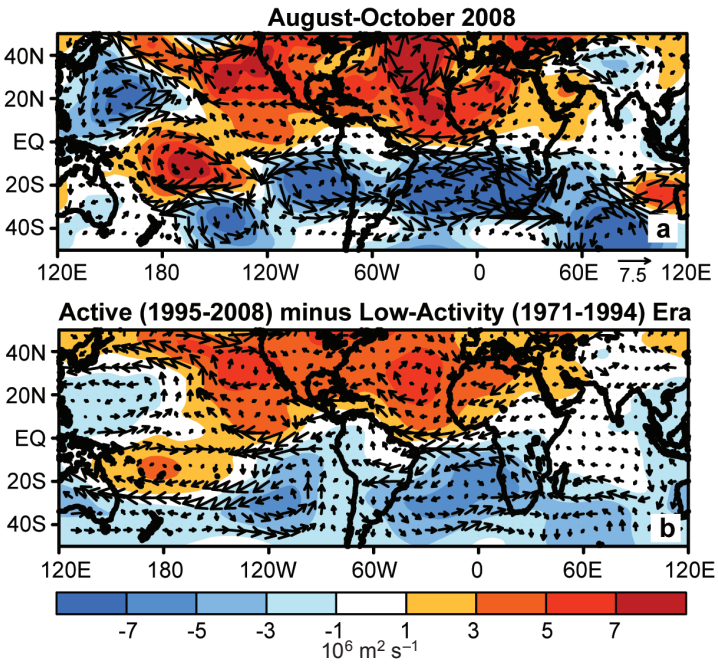

Fig. 4.14. 200-hPa streamfunction (shading) and vector wind (m s^{-1}): (a) Aug–Oct 2008 anomalies and (b) high-activity (1995–2008) period means minus low-activity (1971–94) period means. In (a), anomalous ridges are indicated by positive values (red) in the NH and negative values (blue) in the SH. Anomalous troughs are indicated by negative values in the NH and positive values in the SH. Anomalies are departures from the 1971–2000 monthly means.

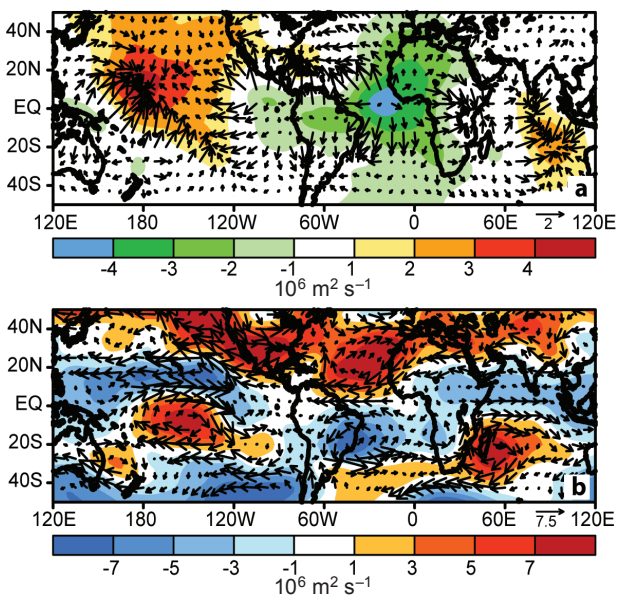

Fig. 4.15. Apr–Jun 2008 anomalies at 200 hPa: (a) velocity potential (shading) and divergent wind vectors (m s^{-1}) and (b) streamfunction and total wind vectors (m s^{-1}). In (b), anomalous ridges are indicated by positive values (red) in the NH and negative values (blue) in the SH. Anomalous troughs are indicated by negative values in the NH and positive values in the SH. Anomalies are departures from the 1971–2000 monthly means.

3) Eastern North Pacific basin—M. C. Kruk, D. H. Levinson, and J. Weyman

(i) Seasonal activity

The ENP basin includes two regions officially designated by NOAA's NWS for issuing NS and H warnings and advisories. The ENP warning area extends from the West Coast of North America to 140°W and is the responsibility of NOAA's NHC in Miami, Florida, while the central Pacific warning area between 140°W and 180° is the responsibility of the CPHC in Honolulu, Hawaii. The 2008 TC activity in both these warning areas is covered using combined statistics, along with information summarizing activity and impacts in the central North Pacific region.

The ENP hurricane season officially lasts from 15 May to 30 November. The peak activity for the central (eastern) part of the region normally occurs in August (September). The 2008 ENP hurricane season produced 17 NSs, 7 Hs, and 2 MHs (Fig. 4.16a). These values are generally below the 1971–2005 averages of 16.2 NSs, 9.1 Hs, and 4.3 MHs.

The 2008 season began on schedule with NS Alma (29–30 May), which was also the first NS to develop east of 90°W since 1970. For the season as a whole, the number of NSs that developed was above average, although few of these systems became hurricanes. As a result, the seasonal ACE (Bell et al. 2000; Bell and Chelliah 2006) was only 81.4 × 10^4 kt^2, which was shy of the 1971–2005 mean (126.3 × 10^4 kt^2) but higher than occurred during the 2007 season (Fig. 4.16b).

Only one system (Kika) was observed in the central North Pacific region during 2008, which is well below the 1971–2005 average of 4–5 TCs.[1] TS Kika entered the region from the east and stayed well south of the Hawaiian Islands before dissipating.

(ii) Historical context of the 2008 ENP hurricane season

Since 1995, the number of NSs in the ENP basin has been near average, fluctuating around the long-term mean (Fig. 4.16a). However, the numbers of Hs and MHs have been generally below normal, with above-normal H activity seen in only two seasons

[1] CPHC includes TDs in its climatological statistics for the central North Pacific region.

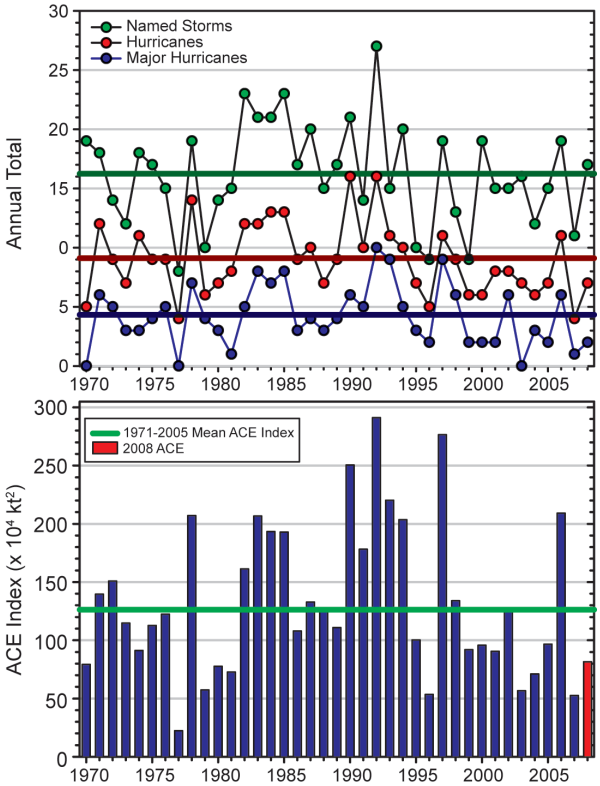

Fig. 4.16. Seasonal TC statistics for the east North Pacific Ocean during 1970–2008: (a) number of NS, H, and MH and (b) ACE (× 10^4 kt^2) with the seasonal total for 2008 highlighted in red. Both time series include the 1971–2005 base period means.

(2000 and 2006). NOAA has identified 9 of the 14 ENP seasons during 1995–2008 as being below normal, with only the 1997 and 2006 El Niño–influenced seasons producing above-normal activity as measured by ACE. In contrast, higher activity seen during the preceding 1970–94 period had 6 of 25 (24%) below-normal seasons and 9 of 25 (36%) above-normal seasons as measured by ACE.

These active and inactive ENP eras are opposite to those observed over the North Atlantic. Such east–west oscillations in activity reflect the large-scale atmospheric circulation anomalies that extend across both basins (Bell and Chelliah 2006). The spatial scale of these atmospheric anomalies is far larger than the area of warmer Atlantic SSTs (Lander and Guard 1998; Landsea et al. 1998, 1999; Goldenberg et al. 2001), suggesting this warmth alone is not a primary direct cause for the 1995 transition to generally below-normal (above normal) ENP (Atlantic) hurricane seasons.

(iii) Environmental influences on the 2008 season

Seasonal TC activity (both frequency and intensity) in the ENP basin is influenced by several large-scale environmental factors, including SSTs, 200–850-hPa vertical wind shear, the phase of the ENSO in the equatorial Pacific region (Whitney and Hobgood 1997), and possibly the phase of the equatorial QBO in the tropical lower stratosphere. ENSO is known to strongly modulate both the SSTs and vertical wind shear on seasonal time scales (Whitney and Hobgood 1997). Multidecadal fluctuations in ENP activity are less well understood, but they show a strong relationship to the phase of the tropical multidecadal signal (Bell and Chelliah 2006) and Atlantic hurricane activity.

El Niño typically favors an above-normal ENP season, while La Niña favors a below-normal season (Irwin and Davis 1999; Frank and Young 2007; Camargo et al. 2008). These ENSO impacts are modulated by the multidecadal signal, with the combination of La Niña during an inactive hurricane era greatly increasing the probability of a below-normal season. During 2008, the weakening state of La Niña to a more neutral phase during the climatological peak of the hurricane season (August–October) resulted in near-average SSTs (−0.5° to +0.5°C anomalies) in the MDR[2] during most of the season (Figs. 4.2c,d). In the absence of a strong ENSO signal, neutral years tend to favor below-normal hurricane activity in the ENP.

Another contributing factor to the below-normal season was above-average vertical wind shear between 200 and 850 hPa in the MDR during JJA (Fig. 4.17a). The largest shear anomalies (exceeding 9–12 m s^{-1}) were observed during JJA (Fig. 4.17a), followed by negative anomalies of 6–12 m s^{-1} during SON (Fig. 4.17b). This stronger-than-normal shear early in the season likely prevented systems from intensifying very quickly, and as a result 2008 had shorter-lasting and fewer-than-average Hs and MHs.

Previous studies have shown some statistically significant correlations between ENP hurricane activity and the phase of the QBO (Gray 1984; Shapiro 1989; Whitney and Hobgood 1997). In the ENP, TCs may attain a higher intensity when the QBO is in its westerly phase at 30 hPa, but there is also a corresponding decrease in the observed seasonal frequency (Whitney and Hobgood 1997). During May, the phase of the QBO was westerly, as indicated by westerly winds at 30 and 50 hPa. The winds were again westerly at both levels in June, and thereafter

[2] For the eastern North Pacific basin the MDR covers the area 10°–20°N and 90°–130°W (green boxes, Fig. 4.17).

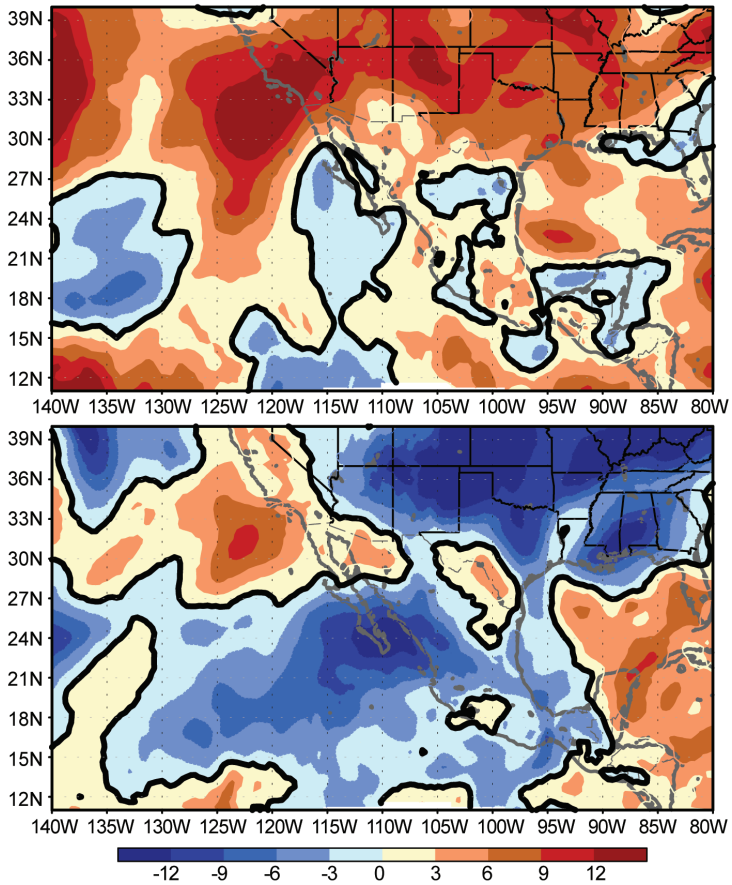

Fig. 4.17. The 200–850-hPa vertical wind shear anomaly (m s^{-1}) during (top) Jun–Aug and (bottom) Sep–Nov 2008. Anomalies are departures from the 1979–2004 period means. (Source: NOAA NOMADS NARR dataset.)

remained constant throughout the remainder of the hurricane season (not shown). Therefore, the westerly phase of the QBO may have aided in allowing more TCs to develop in the ENP basin in 2008.

(iv) Tropical cyclone impacts in 2008

Three TSs made landfall along the Pacific coast of Mexico during 2008 [NS Julio, NS Lowell (as a tropical depression), and Category-2 H Norbert]. This is well above the 1951–2000 average of 1.34 landfalling TSs and near the average of 1.3 landfalling Hs (Jauregui 2003).

In Central America, NS Alma made landfall along the northwestern coast of Nicaragua on 29 May with maximum sustained winds of 55 kt. The wind and rain from NS Alma forced the evacuation of 25,000 residents, and many homes were destroyed and flooded.

On 23 August, NS Julio made landfall on the coast of Mexico with maximum sustained winds of 40 kt and moved northwestward paralleling the coastline. Two persons were killed in the southern tip of Baja California by the heavy rains and flash flooding. Roughly two weeks later, NS Lowell made landfall in Baja California on 11 September. No significant damage was caused by the excessive rains from Lowell, which had peak winds near 30 kt at landfall.

The strongest storm of the ENP 2008 season was Category-4 MH Norbert, which made landfall in Baja California on 11 October as a Category-2 H, and again as a Category-1 H in Sonora, Mexico. Maximum sustained winds during Norbert's peak intensity were measured at 115 kt, becoming only the second MH of the ENP 2008 season (after Category-3 MH Hernan, which remained over the open waters). MH Norbert was the first October hurricane to strike the western Baja California peninsula since H Pauline (1968). MH Norbert was responsible for five deaths as it made landfall in Mexico.

There was no direct landfall or strike associated with NS Kika (7–12 August) in the central North Pacific. Kika formed east of 150°W and moved westward before dissipating near 165°W. Maximum sustained winds from NS Kika topped out at 35 kt as it stayed over open waters, well south of Hawaii.

4) Western North Pacific basin—S. J. Camargo

The 2008 season featured 27 TCs, with 25 reaching TS intensity (though 4 were not named), 12 becoming TYs, and only 2 reaching STY intensity (see Fig. 4.18a). TC data are from the JTWC, and the climatology is defined as 1971–2000.

There were significant differences between the 2008 warnings by JTWC and the RSMC in Tokyo. The RSMC did not name four TCs that the JTWC considered to have reached TS intensity (01W, 14W, 16W, and 22W). Halong was considered a TY by JTWC, but not by Tokyo. In contrast, Phanfone was considered a TS by RSMC, but not by JTWC (Chan 2009).

The 2008 season started in January with unnamed TS (01W). In April, TY Neoguri was the earliest TY to make landfall in China in the historical record.[3] There was a historical record number of TYs (three)

[3] China Meteorological Agency statement in the Chinese media.

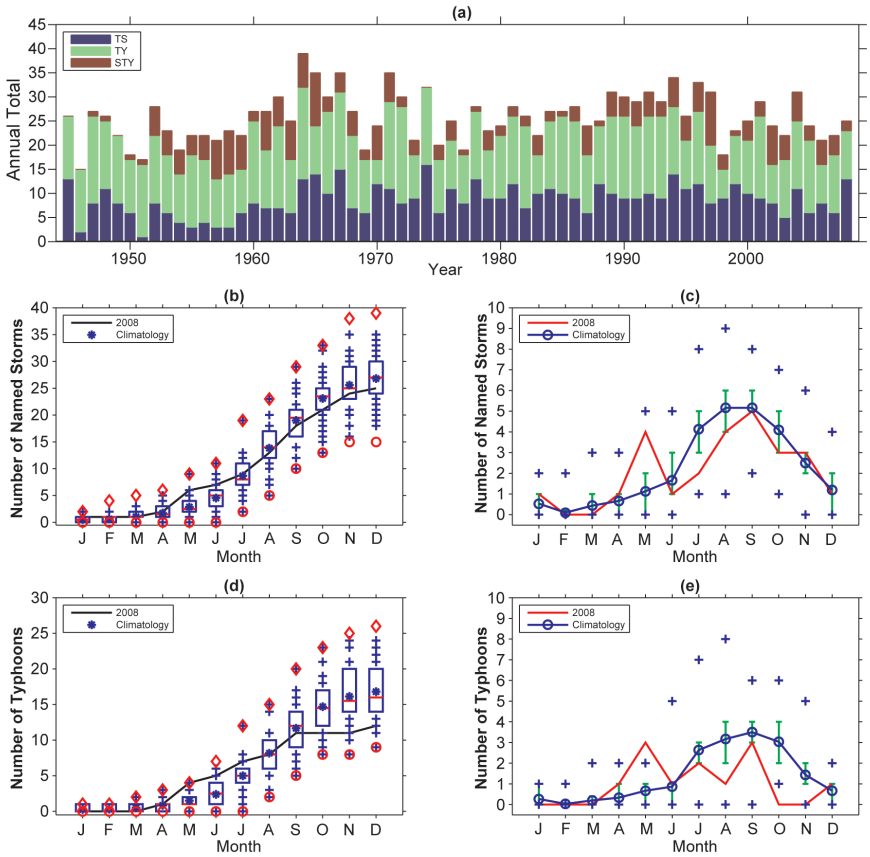

Fig. 4.18. (a) Number of TSs, TYs, and STYs per year in the WNP 1945–2008. (b) Cumulative number of TCs with TS intensity or higher (NS) per month in the WNP: 2008 (black line) and climatology (1971–2000) shown as box plots [interquartile range: box, median; red line, mean; blue asterisk, values in the top or bottom quartile; blue crosses, high (low) records in the 1945–2006 period; red diamonds (circles)]. (c) Number of NSs per month in 2008 (black curve); mean climatological number of NSs per month (blue curve); the blue plus signs denote the maximum and minimum monthly historical values (1945–2008); and green error bars show the interquartile range for each month. In the case of no error bars, the upper and/or lower percentiles coincide with the median. (d) Cumulative number of TYs per month in the western North Pacific: 2008 (black line) and climatology (1971–2000) shown as box plots. (e) Number of TYs per month in 2008 (black curve); mean climatological number of TY per month (blue curve); the blue plus signs denote the maximum and minimum monthly historical values (1945–2008); and green error bars show the interquartile range for each month. (Source: 1945–2007 JTWC best-track dataset, 2008 JTWC preliminary operational track data.)

in May (Fig. 4.18e, climatological median 1), including STY Jangmi. June, July, and August featured TSs and TYs in the bottom quartile of the distribution. The number of NSs in September was equal to the climatological median, but the number of TYs was in the bottom quartile of the distribution. October 2008 was the first October in the historical record with no TYs (climatological median is 3). The previous record was October 1976, with one STY. In November, three TSs occurred. TY Dolphin, in December, closed the 2008 season (see sidebar "Unusually Quiet West Pacific Typhoon Season Ends with a Dolphin Kick").

The total number of TCs, TYs, and STYs were all in the bottom quartile of the climatological distributions (median: 30.5 TCs, 16 TYs, and 3 STYs). The number of TSs was below the median (27). The cumulative distribution of NSs (Figs. 4.18b,d) shows above-normal activity in the early season, and below-normal activity for the rest of the season, especially for TYs. The number of TYs in 2008 is in the lowest 15th percentile. The number of NSs in the season was only slightly below the median. The number of STYs in 2008 (two) was in the bottom quartile of the distribution (median is 3). The low activity in 2008 is therefore mainly due to lack of intensification of the TCs to TY intensity.

The 2008 ACE (Bell 2000) was below the bottom 15th percentile of the climatological distribution (Fig. 4.19a). Reflecting the occurrence of TYs, the ACE for the early season (April–June) was in the top 10th percentile of the distribution (Fig. 4.19b), while the ACE for the peak season (July–October) was in the bottom 5th percentile. The ACE value in May was in the top quartile, mainly due to the occurrence of STY Rammasun (77% of the May ACE value). September was the only peak-season month with an ACE value near the climatological median. STY Jangmi (30% of September ACE) was the most intense TY in 2008 with peak winds near 135 kt.

There is a known relationship between ACE and ENSO, with low values of ACE usually occurring in La Niña years, when the TCs tend to be short lived

and less intense (Wang and Chan 2002; Camargo and Sobel 2005; Camargo et al. 2007a). According to the Niño-3.4 and Niño-3 indices, the 2007–08 La Niña ended during the boreal summer and reemerged toward the end of the year. However, in the Niño-4 region, anomalously cool SSTs never warmed, despite the occurrence of warming SSTs in the eastern Pacific (not shown). The Southern Oscillation index was briefly neutral during the summer months but was positive after September. Key TC environmental conditions in the western North Pacific were consistent with La Niña events. Most notably, the eastern portion of the monsoon trough was confined to a small region west of the Philippines (Fig. 4.20a) (Camargo et al. 2007a), and the Pacific decadal oscillation was strongly negative throughout 2008.

During 2008, the median duration of NSs was only 4.75 days (bottom 15th percentile of the distribution). The median lifetime of NSs during La Niña is 6.75 days. The duration of 14 TCs was in the bottom quartile of the distribution, and only 2 TCs had lifetimes above the median (8 days). As a result, the number of days with TS was only 92.5 (median is 144.25). There were only 75.5 TY days (median is 120.4) and 9.25 STY days (median is 19.4 days), both in the bottom quartiles of the distributions.

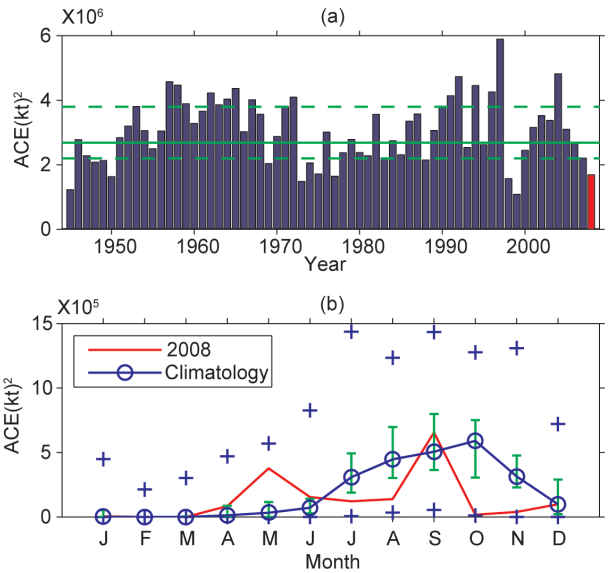

Fig. 4.19. (a) ACE values per year in the WNP for 1945–2008. The solid green line indicates the median for 1971–2000 climatology, and the dashed green lines show the 25th and 75th percentiles. (b) ACE values per month in 2008 (red line) and the median in 1971–2000 (blue line), where the green error bars indicate the 25th and 75th percentiles. In the case of no error bars, the upper and/or lower percentiles coincide with the median. The blue plus signs denote the maximum and minimum values during the period 1945–2008. (Source: 1945–2007 JTWC best-track dataset, 2008 JTWC preliminary operational track data.)

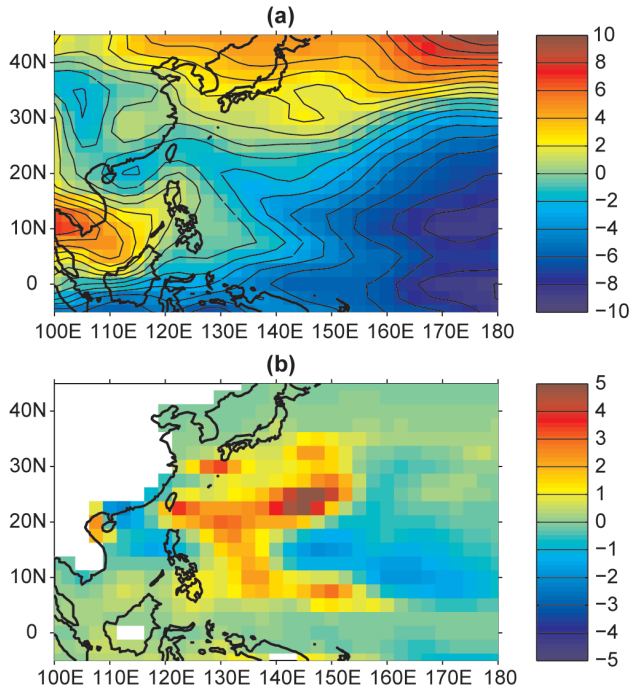

Fig. 4.20. (a) Zonal 850-hPa winds (m s^{-1}) from JASO 2008. The contour interval is 1 m s^{-1}. (b) Genesis potential index (Camargo et al. 2007b) anomalies for JASO 2008. (Source: atmospheric variables—NCEP reanalysis data; Kalnay et al. 1996; SST—Smith and Reynolds 2005.)

Fourteen TCs made landfall during 2008, which is just below the 1951–2000 median of 15.[4] Two systems made landfall as a TD (median is 3), six made landfall as a TS (median is 6), six struck as a TY (median is 4), and none as a STY (median is 0).

The Philippines were affected by four TCs in 2008: TYs Neoguri and Fengshen, and TSs Halong and Higos. The largest impacts resulted from TY Fengsheng, which brought more than 1,300 deaths.

Taiwan was hit by four TYs in 2008: Kaelmaegi and Fung-wong in July, and Sinlaku and Jangmi in September. They brought heavy rainfall amounts to Taiwan, causing large losses to agriculture and infrastructure. Both TYs Kaemaegi and Fung-wong also affected mainland China, after crossing Taiwan and becoming weaker. TYs Kammuri, Nuri, and Hagupit and TS Higos also made landfall in China. Vietnam

[4] Here we consider only one landfall per TC. If a TC makes more than one landfall, the landfall event with the highest wind speed is considered.

was also affected in this typhoon season, with three landfalls (TS Mekkhala, 22W, and Noul).

The GPI (Emanuel and Nolan 2004) during 2008 was above normal in the western portion of the WNP and below normal near the date line and in the South China Sea (Fig. 4.20b), which is also consistent with the presence of La Niña (Camargo et al. 2007b). The decreased GPI near the date line in La Niña events is mainly attributed to the low-level vorticity, while the increased GPI near the Asian continent is attributed to an increase in midlevel relative humidity (Camargo et al. 2007b).

5) Indian Ocean basins—K. L. Gleason and M. C. Kruk

(i) NIO

The NIO TC season typically extends from April to December, with two peaks in activity during May–June and November when the monsoon trough is positioned over tropical waters in the basin. TCs in the NIO basin normally develop over the Arabian Sea and Bay of Bengal between latitudes 8° and 15°N. These systems are usually short lived and relatively weak, and they often quickly move into the Indian subcontinent. However, strong and "severe cyclonic storms"[5] can develop with winds exceeding 130 kt (Neumann et al. 1993).

The 2008 TC season produced seven NSs, one CYC, and one MCYC (Fig. 4.21a). These values are near the 1981–2005 averages of 4.6 NSs, 1.4 CYCs, and 0.5 MCYCs. The season produced an ACE value of 19×10^4 kt^2, which is slightly above the 1981–2005 mean of 16×10^4 kt^2 (Fig. 4.21b).

The 2008 season was most noted for MCYC Nargis, which made landfall on the Irrawaddy Delta of Myanmar on 2 May. Nargis began as a disturbance east of the Nicobar Islands on 24 April. As it migrated to the northwest, it entered a region of low vertical wind shear and began to intensify. By 28 April, Nargis was a Category-1 CYC and continued to intensify as it turned toward the Myanmar coast. The storm rapidly intensified over a period of 24 h (1–2 May), with peak maximum sustained winds reaching 115 kt. This storm caused catastrophic destruction and significant loss of life, with estimates of 146,000 fatalities and thousands missing. The massive storm surge inundated the low-lying coastal region and was the reason for the majority of the fatalities. Extreme winds and high storm surge were responsible for damage estimates of over $10 billion (USD). MCYC Nargis was the most damaging cyclone recorded in this basin and the seventh-deadliest cyclone of all time.

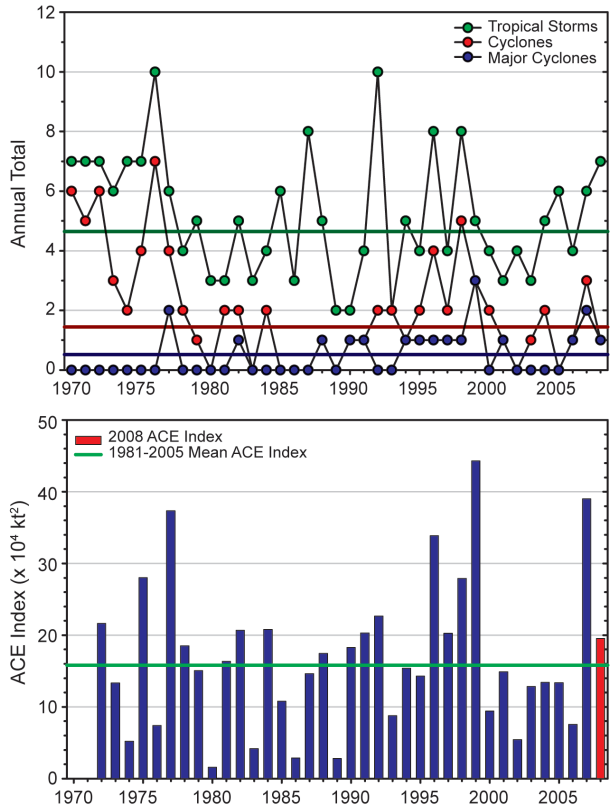

Fig. 4.21. Annual TC statistics for the NIO over the period 1970–2008: (a) number of TSs, CYCs, and MCYCs, and (b) the estimated annual ACE ($\times 10^4$ kt^2) for all TCs during which they were at least TS or greater intensities (Bell et al. 2000). The 1981–2005 base period means are included in both (a) and (b). Note that the ACE values are estimated due to a lack of consistent 6-h-sustained winds for every storm.

(ii) Southern Indian Ocean

The SIO basin extends south of the equator from the African coastline to 105°E, with most CYCs developing south of 10°S. The SIO TC season extends from July to June encompassing equal portions of two calendar years (e.g., the 2008 season is composed of storms from July to December 2007, and January to June 2008). The peak activity occurs during December–April when the ITCZ is located in the Southern Hemisphere and is migrating equatorward. Historically, the vast majority of the landfalling CYCs in the SIO impact Madagascar, Mozambique, and the Mascarene Islands, including Mauritius and Réunion.

[5] The Bangladesh Supercyclone of 1970 produced perhaps the greatest human death toll (300,000 persons) on record, primarily from storm surge flooding of low-lying deltas (Holland 1993).

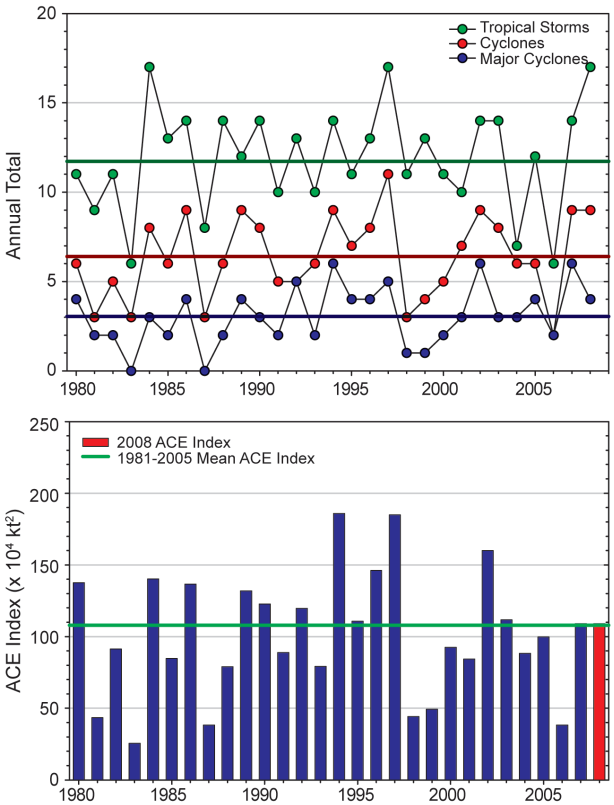

Fig. 4.22. Same as in Fig. 4.21, but for TCs in the SIO over the period 1980–2008.

The historical SIO TC data are probably the least reliable of all the TC basins (Atkinson 1971; Neumann et al. 1993), primarily due to a lack of historical record keeping by individual countries and no centralized monitoring agency; however, the historical dataset for the region has been updated (Kruk et al. 2009, manuscript submitted to *J. Atmos. Oceanic Technol.*; Knapp et al. 2009). The historical data are noticeably deficient before reliable satellite data were operationally implemented in the region beginning about 1983.

The 2007–08 season produced 17 NSs and above-average numbers of CYCs (9) and MCYCs (4) (Fig. 4.22a). The 1981–2005 averages are 11.8 NSs, 6.4 CYCs, and 3 MCYCs. However, the 2007–08 ACE (109 $\times 10^4$ kt^2) was near the 1981–2005 average (Fig. 4.22b). Over the last 10 years, only the 2001–02 season had above-average ACE. Previous to that, the most recent period with above-average ACE occurred during the period from 1994 to 1997.

The strongest storm during the 2007–08 season was MCYC Hondo, which reached peak strength of 125 kt on 7 February. Hondo formed approximately 560 nm southeast of Diego Garcia on 4 February and began rapid intensification early the next day. As it migrated south over the central Indian Ocean, it continued to organize into a Category-4 MCYC. Over the next couple of days, MCYC Hondo entered a region of higher wind shear and cooler ocean waters and began to weaken.

The strongest landfalling storm of the season formed off the northeast coast of Madagascar on 7 February. The disturbance quickly intensified into CYC Ivan before tracking to the southeast and again entered a region with unfavorable wind shear. After some weakening and meandering, Ivan regained its strength and began a southwestward track toward the east coast of Madagascar. At peak intensity, MCYC Ivan had sustained winds of 115 kt and made landfall north of Fanoarivo, Madagascar, on 17 February. Nearly 100 fatalities were reported and over 330,000 residents were rendered homeless. Damages from Ivan were estimated at more than $30 million (USD).

6) Southwest Pacific basin—M. J. Salinger

The 2007–08 southwest Pacific TC season had 4 TC occurrences (east of 150°E), 5 less than the median of 9 (1976–77 to 2006–07) for the region in the TC season (Fig. 4.23). The first TC of the season occurred on 3 December. The season finished unusually early with the last in late January/early February (the TC season typically runs into May).

The season's NSs were clustered nearer the date line in the southwest Pacific region, with three tracking near Fiji (Fig. 4.24). Rather than the normal February–March peak, the season peaked early, with three of the four NSs forming in January and the remainder of the season being unusually quiet. Three of the four TCs in the southwest Pacific region reached H strength, and two reached MH strength.

TC Daman was the first of the season, occurring 5–9 December near Fiji, with maximum sustained winds of 105 kt. Daman produced heavy rainfall over northern Fiji, with destructive winds flattening vil-

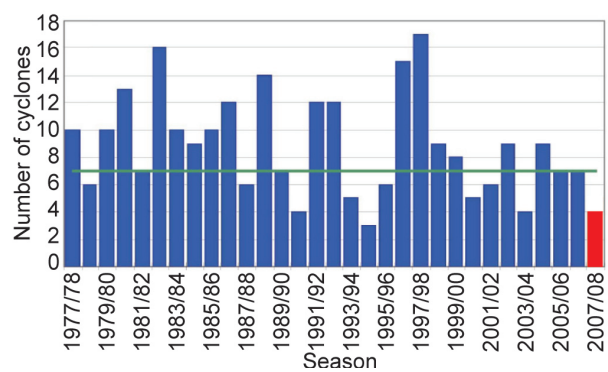

Fig. 4.23. TC frequencies in the southwest Pacific, 1976–2008.

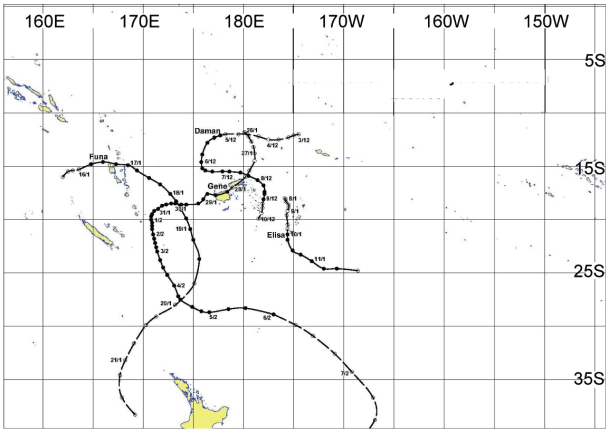

Fig. 4.24. TC tracks in the Southwest Pacific, 2007–08.

lages and causing widespread destruction to roads and property. TC Elisa formed on 10 January near the date line and moved southwest of Nukualofa, Tonga, producing maximum sustained winds of 45 kt. TC Funa developed near Fiji, then moved southeast toward Tonga 16–19 January with maximum sustained winds of 105 kt, causing heavy rain and storm-force winds to Vanuatu, which disrupted communications. TC Gene was the last of the 2007/08 winter season, developing northeast of Fiji and tracking toward New Caledonia. Maximum sustained winds were near 100 kt. This storm caused seven deaths on Fiji, left many without power, and caused estimated damages of $25 million (USD).

7) Australian basin—B. Trewin and A. B. Watkins

(i) Seasonal activity

The 2007–08 TC season was near normal in the broader Australian basin (areas south of the equator and between 90° and 160°E,[6] which includes Australian, PNG, and Indonesian areas of responsibility). The season produced 10 TCs, equal to the long-term average. There were three TCs in the eastern sector[7] of the Australian region during 2007–08, and seven TCs in the western sector. The number of landfalls was relatively low, with only two landfalls during the season.

(ii) Landfalling and other significant TCs

The most intense TC during the season was TC Pancho, which formed off the northwest coast on 25 March. It reached peak intensity (Category-4, 95-kt sustained winds with 135-kt gusts, 934-hPa central pressure; see www.bom.gov.au/weather/cyclone/faq/index.shtml for a definition of Australian TC categories) at 0000 UTC 27 March. It weakened below TC intensity before making landfall as a tropical low near Shark Bay on 29 March, bringing heavy rain to parts of southwestern Western Australia. An intense midlatitude low that absorbed the remnants of Pancho was responsible for widespread wind damage in Victoria and Tasmania on 2 April.

TC Nicholas was the sole landfalling TC in the western sector. It formed on 12 February and peaked as a Category-3 system (80-kt sustained winds with 115-kt gusts, central pressure 948 hPa) on 16–17 February. It eventually crossed the coast south of Coral Bay as a Category-1 system on 20 February. No significant damage was reported on land, but widespread shutdowns of the offshore oil and gas industry resulted in economic losses of several hundred million USD.

The other landfalling system of the season was TC Helen, which formed off the west coast of the top end of the Northern Territory and made landfall on 4 January about 100 km southwest of Darwin as a Category-2 system (50-kt sustained winds with 65-kt gusts, central pressure 975 hPa). There was some minor wind damage in the Darwin area. While Helen was short lived as a TC, long-lived remnants of the system moved into Queensland and contributed to major flooding in central Queensland in mid-January. Helen's track was also unusual, being the first landfall from the west on the top end coastline since Tracy in 1974–75.

TC Guba, which moved over waters east of Queensland from 14 to 20 November (2007) and peaked as a Category-3 system, was significant in that it approached the Queensland coast more closely than any other recorded November cyclone, although it did not ultimately make landfall. Guba's antecedent low caused severe flooding, with numerous deaths, in PNG on 12–13 November.

e. *Intertropical Convergence Zones*

1) Pacific—A. B. Mullan

There are two prominent convergence zones in the Pacific: the ITCZ in the Northern Hemisphere, which lies approximately parallel to the equator, with its position varying seasonally from around 5° to 7°N in February–May to 7° to 10°N in August–November

[6] The Australian Bureau of Meteorology's warning area overlaps both the SIO and SWP.

[7] The western sector covers areas between 90° and 125°E. The eastern sector covers areas east of the eastern Australian coast to 160°E, as well as the eastern half of the Gulf of Carpentaria. The northern sector covers areas from 125° E east to the western half of the Gulf of Carpentaria.

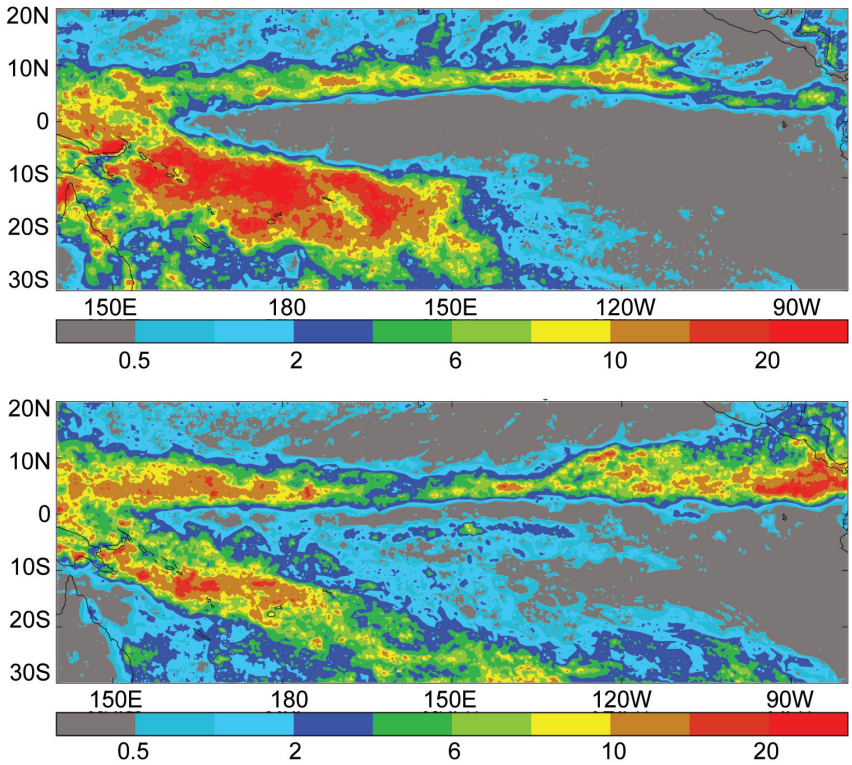

Fig. 4.25. Annual average rainfall rate from TRMM 0.25° analysis for (top) Jan 2008 and (bottom) May 2008. Note the uneven contour intervals (0.5, 1, 2, 4, 6, 8, 10, 15, and 20 mm day^{-1}).

(Fig. 4.27); and the SPCZ, which extends diagonally from around Solomon Islands (10°S, 160°E) to near 30°S, 140°W, and is most active in the November–April half-year.

Figure 4.25 shows the monthly rainfall in the tropical Pacific for two selected months in 2008, as derived from the 0.25° resolution NASA TRMM rainfall data (3B-43 product; Huffman et al. 2007). The year 2008 began with a continuation of strong to moderate La Niña conditions, and the January 2008 rainfall shows a clear separation between the ITCZ and SPCZ around the date line, with a region of suppressed convection extending from western to eastern Kiribati, which resulted in low rainfall in the northern Cooks and the Marquesas of French Polynesia. The SPCZ was well south and west of its normal position and very active through the first quarter of 2008 (Fig. 4.26, left), resulting in much-above-average rainfall in Vanuatu, New Caledonia, Tonga, Niue, and southern Cooks.

In May (Fig. 4.25, bottom), the SPCZ was still active and south of its normal position. A very clear southern branch of the ITCZ is apparent between 180° and 120°W, while the ITCZ in the Northern Hemisphere appears somewhat weaker than usual over the same longitudes. To the north of this section of the ITCZ, there is suppressed convection to at least 20°N, which was typical of the second quarter of 2008, contributing to the drought conditions that were declared in many parts of the Hawaiian Islands by midyear. The May rainfall also highlights a more intense ITCZ around 90°W. This continued into October, coinciding with several months of above-normal SSTs in the far eastern equatorial Pacific.

Unusually persistent trade winds dominated the weather across Micronesia and the equatorial South Pacific during the third quarter of 2008 (Pacific ENSO Applications Center 2008; Island Climate Update 2008b,c), and the ITCZ lay on the equatorward edge of its climatological distribution (Fig. 4.26, right). The SPCZ was fairly inactive in the third quarter, but convective activity increased in October and the SPCZ ended the year as it began—south of its normal position. The ITCZ spent much of the year, April through November (Figs. 4.26, right, 4.27), equatorward of its normal position, especially over the central Pacific (180° to 120°W).

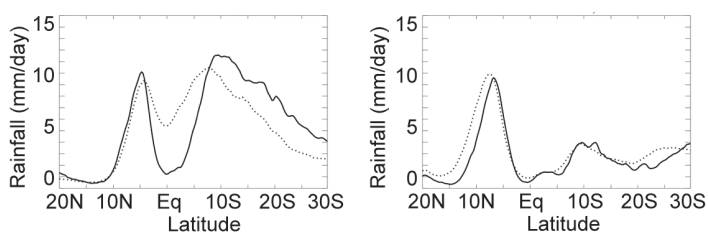

Fig. 4.26. Latitudinal cross-sections of TRMM rainfall (mm day^{-1}): Jan to Mar quarter averaged across the sector (left) 150°E–180°, and Jul to Sep quarter averaged across the sector (right) 180°–150°W. Profiles are given for 2008 (solid line) and the 1998–2007 average (dotted line).

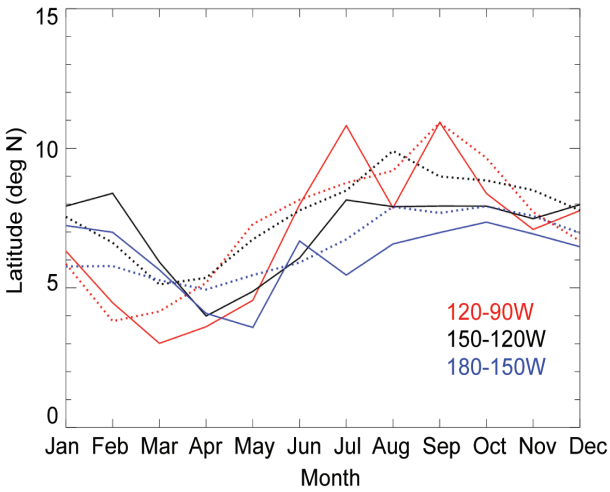

Fig. 4.27. Monthly variation in latitude of peak ITCZ rainfall over three longitude sectors: 180°–150°W (blue), 150°–120°W (black) and 120°–90°W (red). Annual cycle variations given for 2008 (solid lines) and the 1998–2007 climatology (dotted).

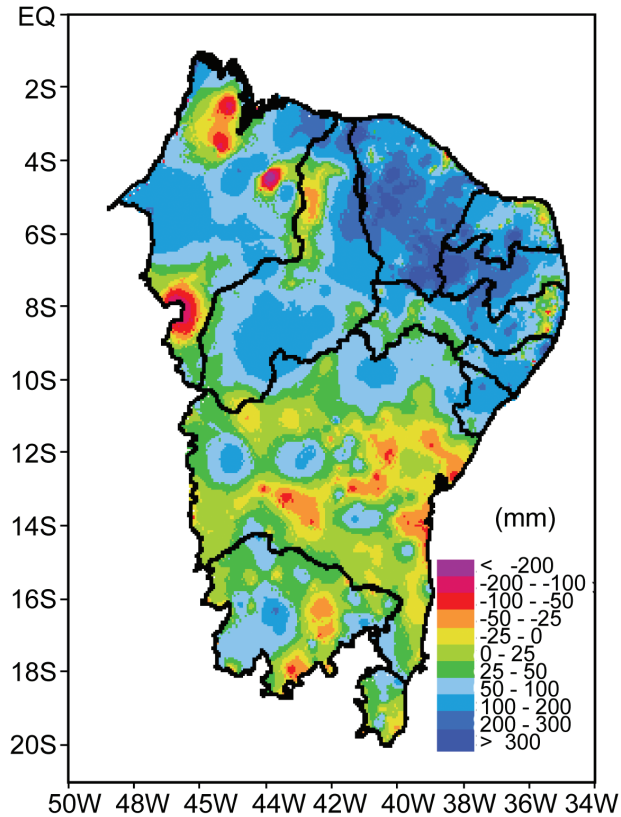

Fig. 4.28. Northeastern Brazil Mar 2008 precipitation anomalies (mm) with respect to 1961–90 climatology based on high-resolution station data.

2) Atlantic—A. B. Pezza and C. A. S. Coelho

The Atlantic ITCZ is a well-organized convective band that oscillates approximately between 5° and 12°N during July–November and 5°N and 5°S during January–May (Waliser and Gautier 1993; Nobre and Shukla 1996). As equatorial Kelvin waves can modulate the ITCZ's interannual variability, ENSO is also known to influence it on a seasonal scale (Münnich and Neelin 2005).

In the semiarid area of northeastern Brazil a sudden southward burst of the Atlantic ITCZ can produce heavy rains (monthly anomalies above 300 mm) as observed in March 2008 (Fig. 4.28). This pattern is facilitated during La Niña and when the South Atlantic is predominantly warmer than the North Atlantic Ocean, as observed in the first half of 2008.

The Atlantic ITCZ reached its southernmost annual position (5°S) during the second half of March in 2008 (Fig. 4.29a). This positioning is within the climatological range (Waliser and Gautier 1993). The ITCZ then migrated rapidly back to the North Atlantic from May (Fig. 4.29b), reaching its northernmost position (10°–15°N) during late August in association with intense convective activity near the African coast (Fig. 4.29c). The resulting convective band during the boreal summer was aligned from southwest–northeast over the North Atlantic (Fig. 4.29c), different from the quasihorizontal alignment observed in May (Fig. 4.29b). This pattern was modulated by strong low-level wind anomalies demarcating the mass convergence between South America and Africa, and further reinforced by a semistationary upper-level vortex over the South Atlantic near northeastern Brazil in August.

For the remainder of the year the Atlantic ITCZ was close to its climatological average, slowly returning to the south and reaching 5°S in December. As a result, a large area of the tropical South Atlantic recorded above-average rainfall in 2008 compared to the 1998–2007 annual mean (Fig. 4.30), contrasting with the below-normal conditions observed in 2006 and 2007.

f. Indian Ocean Dipole—J. J. Luo

The IOD is a coupled ocean–atmosphere phenomenon in the tropical IO. Following a weak negative IOD in 2005, three consecutive positive IODs occurred from 2006 to 2008 (Fig. 4.31a). The SSTs have warmed persistently (Fig. 4.31b) in the central equatorial IO. In contrast, SSTs along the west coast of Sumatra have not increased and are slightly cooler. This indicates the impact of frequent positive IOD on the long-term climatological SST state. The trends of warmer SST in the central and western IO and relatively colder SST west of Sumatra may favor the occurrence of positive IOD.

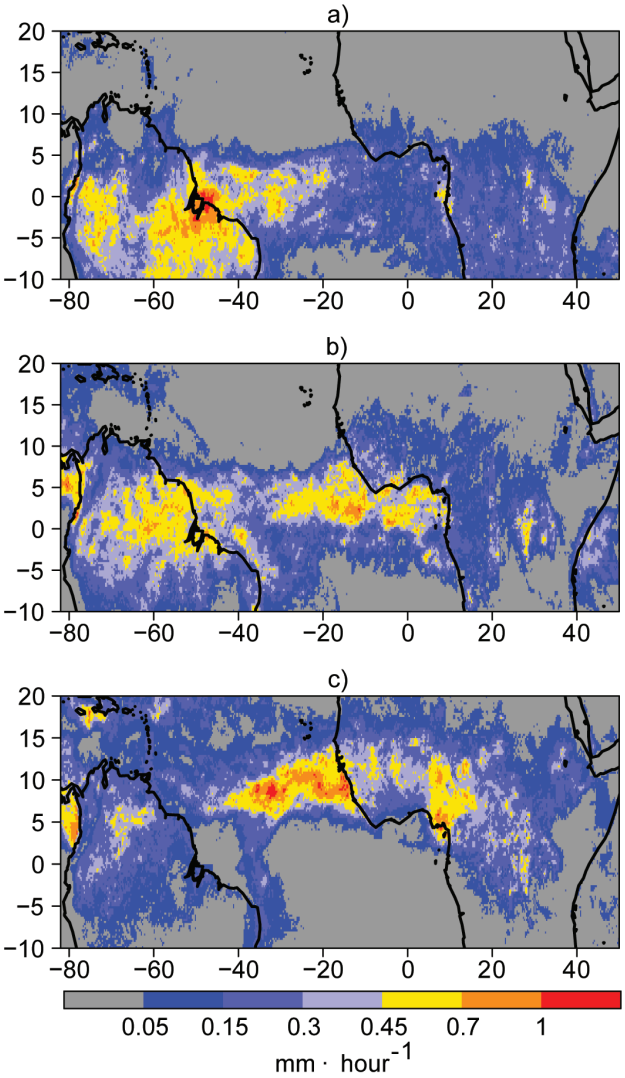

Fig. 4.29. Average rainfall rate (mm h^{-1}) from high-resolution (0.25° lat × 0.25° lon) TRMM analysis for (a) Mar, (b) May, and (c) Aug 2008.

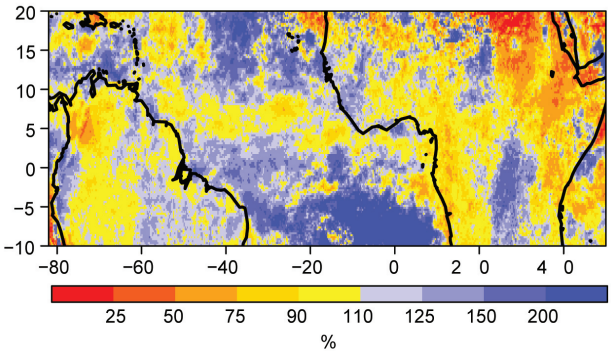

Fig. 4.30. Percentage of the 1998–2007 mean annual rainfall during 2008. Data are TRMM estimates calculated from a 0.25° lat/lon grid.

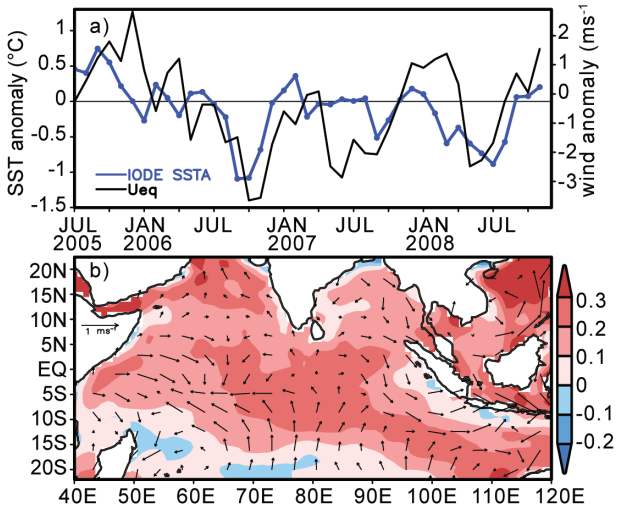

Fig. 4.31. (a) Monthly anomalies of SST (°C) in the eastern pole of IOD (IODE, 90°–110°E, 10°S–0°) and surface zonal wind (m s^{-1}) in the central Indian Ocean (Ueq, 70°–90°E, 5°S–5°N). (b) SST and surface wind differences between the period 1995–2008 and 1982–95. The anomalies were calculated relative to the climatology over the period 1982–2007. These are based on NCEP optimum interpolation SST (Reynolds et al. 2002) and NCEP atmospheric reanalysis data. Here, we used the IODE SST anomaly for IOD definition. Unstable growth of strong surface cooling in this region was found to be closely related to the Bjerknes feedback associated with strong coastal upwelling west of Sumatra, which plays a key role in initiating the positive IOD evolution.

The strong IOD in 2006 coincided with a weak-to-intermediate El Niño, and its evolution is consistent with large-scale IOD dynamics (Luo et al. 2007, 2008). The cold SST anomaly west of Sumatra causes anomalous easterlies in the central Indian Ocean (Fig. 4.31a) in association with the unstable Bjerknes feedback. In contrast, the 2007 weak and short-lived IOD occurred alongside a La Niña (Luo et al. 2008; Luo and Bell 2008). The strong easterlies in the central IO during May–June 2007 played a key role in driving this weak IOD, and in 2008 IOD underwent a unique evolution. During December 2007 to February 2008, anomalous westerlies blew over the IO basin (Fig. 4.32a), particularly between 10°S and the equator, in response to the strong La Niña. Weak cold SST anomalies appeared in the western IO accompanied by weak warming in the east following the demise of the 2007 positive IOD. Correspondingly, more rainfall appeared in the east with drought in the western IO (East Africa). During March–May 2008 (Fig. 4.32b), basin-wide cooling was well developed under the influence of the La Niña. The strong cold

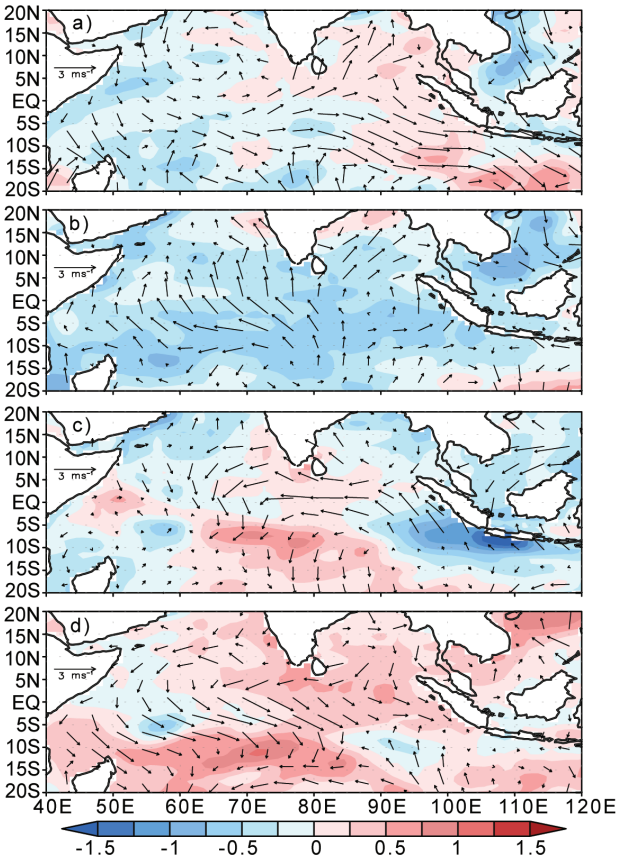

Fig. 4.32. SST (°C) and surface wind anomalies during (a) Dec–Feb 2007–08, (b) Mar–May 2008, (c) Jun–Aug 2008, and (d) Sep–Nov 2008.

SST anomalies in the southwestern IO at 15°–10°S, which caused local drought and anomalous easterlies near the equator, gradually expanded eastward. During May 2008, associated with the arrival of the strong cold SST anomalies and severe drought in the eastern IO at ~10°S, strong equatorial easterly anomalies appeared across the whole basin. This drove an eastward-propagating equatorial upwelling Kelvin wave (Fig. 4.33a) and favored the onset of IOD in the following season.

The positive IOD was well developed during June–August 2008. Strong SST cooling appeared along the west coast of Sumatra with weak warming located in the central IO (Fig. 4.32c). Stronger alongshore southeasterlies enhanced the coastal upwelling and hence favored the development of cold SST and easterly anomalies toward the central Indian Ocean. Such an SST anomaly dipole pattern caused flooding (drought) in the western (eastern) IO. Rainfall over the Indonesia Sea, however, was above normal in association with the La Niña. Due to the IOD influence, Australia again suffered from sustained drought in 2008 despite the prospect of rains resulting from La Niña conditions. During September, the IOD collapsed, in contrast to the usual peak in boreal fall terminating in early winter. Initial westerly wind anomalies appeared in the central equatorial IO during August and intensified in September. This forced a downwelling equatorial Kelvin wave during August–September (Fig. 4.33a) and ended this IOD. During November, the situation in the IO became similar to that during a La Niña year: drought in the west and flooding over the eastern IO, Indonesia, and large parts of Australia.

The concurrence of the positive IOD and La Niña in 2007 and 2008 clearly suggests that potential predictability of IOD may reside in the IO itself. Underlying mechanisms for the 2008 IOD appear to be different from those for the 2006–07 events. Following the demise of the 2007 IOD, a warm subsurface signal persisted in the equatorial eastern IO until May 2008 (Fig. 4.33a). The MJO-related strong cross-basin equatorial easterly anomalies in May appear to have played an important triggering mechanism similar to 2007. Apart from the MJO impact, a clear westward-propagating cold oceanic Rossby wave at 10°–5°S can be seen from November 2007 to May 2008 (Fig. 4.33b). The cold Rossby wave reflected as an eastward-propagating equatorial upwelling Kelvin wave and favored the positive IOD development. Therefore, both the large-scale oceanic process and MJO influences appeared to play important roles in the 2008 IOD development.

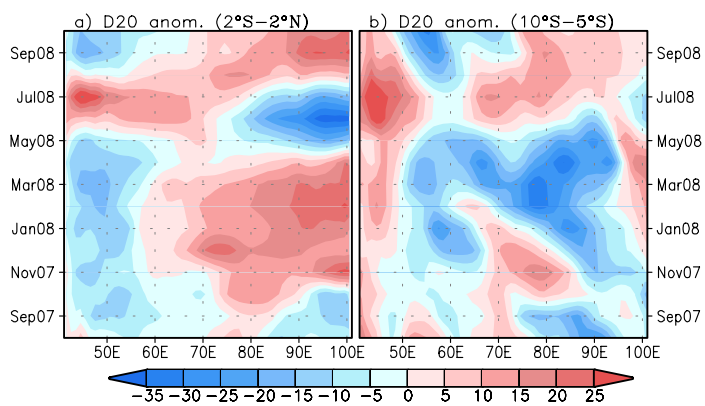

Fig. 4.33. 20°C isotherm depth (D20, m) anomalies in (a) the equatorial Indian Ocean (2°S–2°N) and (b) off-equatorial south Indian Ocean (10°–5°S). The data are derived from the NCEP ocean assimilation system.

UNUSUALLY QUIET WEST PACIFIC TYPHOON SEASON ENDS WITH A DOLPHIN KICK—M. A. LANDER, B. WARD, AND H. J. DIAMOND

In the WNP basin, climatic effects typical of La Niña were noted for much of 2008. These included well-known La Niña–related anomalies such as below-normal TC activity across most of Micronesia, TC activity shifting well to the west and north of normal, a weak (or absent) monsoon, higher-than-normal sea level, and abnormally strong and widespread TW in the lower latitudes (Fig. 4.34).

The 2008 TY season came to an apparent end after STY Jangmi recurved east of Japan in September. There were no TYs in the WNP basin in October for only the second time since JTWC records began in 1959. After the demise of TS Noul in mid-November, TWs of unprecedented persistence and wide coverage seemed to preclude the formation of any more TCs for the remainder of the year. This would have contributed to several statistical extremes of low TC activity in a year, but nature had one more peculiar scenario to play out.

In early December, a midlatitude cyclone east of Japan intensified, matured, and evolved into a warm seclusion. This isolated vortex was then steered southward by a surge of northerly gales. Starting near 30°N, it plunged southward into the deep tropics (12°N), turned west, and became the seed for the season's final TY, Dolphin. Including the early phases of its subtropical existence, Dolphin's track was very unusual (Fig. 4.35).

As Dolphin's seed vortex was driven southward, it was accompanied by an unusual pattern of northerly gale-to-TY-force winds located in the subtropics of the WNP near the date line. These winds generated oceanic swells that traveled southward and caused phenomenal surf at Wake Island, many of the islands and atolls of Micronesia, and the Marshall Islands—and then south to Kiribati, the Solomon Islands, and the northern coast of Papua New Guinea. Breaking surf heights at more than 20 ft were reported on some atolls. Substantial inundation from wave run up was experienced in many locations, with damage to infrastructures, personal property, and crops. Inundation was exacerbated by a combination of extreme wave height, high tides, and high sea levels related to La Niña.

News reports implicated the developing TY Dolphin in the generation of this very high and destructive surf. Dolphin played only a small role in the wave event, but the struggling incipient vortex that became Dolphin defied expectations and intensified to a TS, and then to a TY. As Dolphin intensified, it passed south of Guam, requiring the issuance of the only TC watches and warnings for all of 2008 within the Guam Weather Forecast Office's area of responsibility (equator to 25°N and 130°E to 180°). After passing Guam, it became a TY. It later recurved toward Iwo Jima, Japan, completing an anomalous giant elliptical path (Fig. 4.35) that ended on 19 December near where it had begun on 4 December. After passing Iwo Jima, Dolphin decayed, thus ending this most unusual WNP TY season.

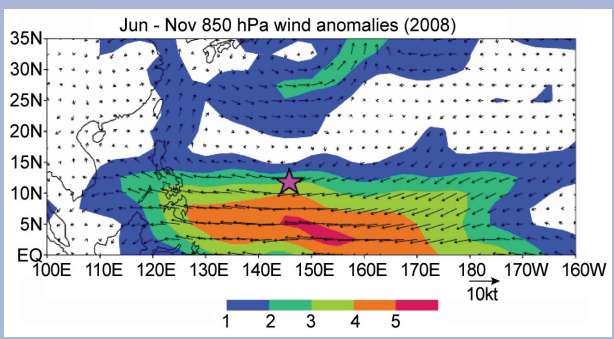

Fig. 4.34. Wind anomaly at 850 hPa for the 6-month period Jun through Nov 2008. This vast easterly wind anomaly in the deep tropics of the western North Pacific was of sufficient magnitude to eliminate the normal monsoon trough of the region and to stifle the normal development of tropical cyclones eastward of the longitude of Guam (purple star). (Figure adapted and used with permission of J–C.L. Chan, City University of Hong Kong.)

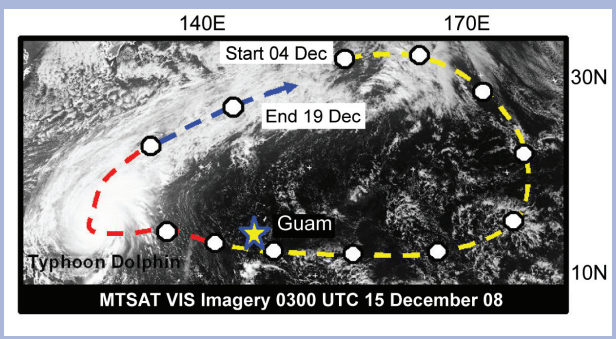

Fig. 4.35. The highly unusual track of TY Dolphin. Filled circles show 24-hr positions, with some circles left out so as not to cover the image of the typhoon. Dolphin is a typhoon in this MTSAT visible imagery of 0300 UTC 15 Dec 2008. Imagery obtained from the geostationary archive of the University of Dundee, U.K. (www.sat.dundee.ac.uk/).